Article

Theoretical Study of Trans-metalation Process in Palladium-Catalyzed Borylation of Iodobenzene with Diboron

Michinori Sumimoto, Naoki Iwane, Tomohiko Takahama, and Shigeyoshi Sakaki

J. Am. Chem. Soc., **2004**, 126 (33), 10457-10471• DOI: 10.1021/ja040020r • Publication Date (Web): 30 July 2004

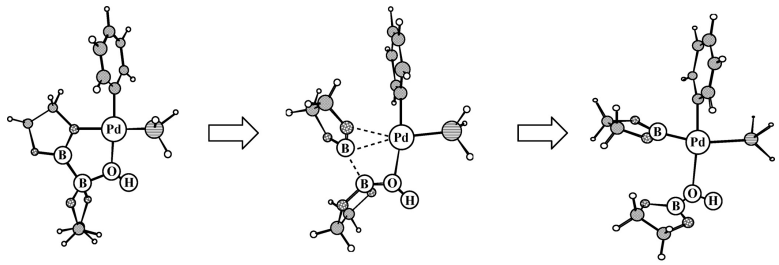

More About This Article

Additional resources and features associated with this article are available within the HTML version:

- Supporting Information
- Links to the 10 articles that cite this article, as of the time of this article download
- Access to high resolution figures
- Links to articles and content related to this article
- Copyright permission to reproduce figures and/or text from this article

View the Full Text HTML

J|A|C|S
ARTICLES
Published on Web 07/30/2004

Theoretical Study of Trans-metalation Process in Palladium-Catalyzed Borylation of Iodobenzene with Diboron

Michinori Sumimoto,† Naoki Iwane,‡ Tomohiko Takahama,‡ and Shigeyoshi Sakaki*,†

Contribution from the Department of Molecular Engineering, Graduate School of Engineering, Kyoto University, Nishikyo-ku, Kyoto 615-8510, Japan and Department of Applied Chemistry and Biochemistry, Faculty of Engineering, Kumamoto University, Kumamoto 860-8555, Japan

Received January 15, 2004; E-mail: sakaki@moleng.kyoto-u.ac.jp

Abstract: Trans-metalation process in the palladium-catalyzed borylation of iodobenzene with diboron was theoretically investigated with the DFT method. Palladium(II) hydroxo phenyl complex, $Pd(OH)(Ph)(PH_3)_2$, and the fluoro analogue easily undergo the trans-metalation with diboron, $B_2(eg)_2$ (eg = $-OCH_2CH_2O-$), to afford $Pd(Ph)(Beg)(PH_3)(HO-Beg)$ and $Pd(Ph)(Beg)(PH_3)(F-Beg)$, respectively, where $B_2(eg)_2$ is adopted as a model of bis(pinacolato)diboron used experimentally. The electron re-distribution in the trans-metalation clearly indicates that the B−B bond scission occurs in a heterolytic manner. In the chloro analogue, $PdCl(Ph)(PH_3)_2$, however, the trans-metalation occurs in a homolytic manner with much difficulty, which is consistent with the experimental result. The significant differences between the chloro complex and the other hydroxo and fluoro complexes are easily interpreted in terms that hydroxo and fluoro ligands can form strongly bonding interaction with $B_2(eg)_2$ but the chloro ligand cannot.

Introduction

Transition-metal catalyzed cross-coupling reaction is very important in organic syntheses and organometallic chemistry,[1−9] because a variety of organic compounds can be synthesized through this reaction. For instance, new C−C bond formation is successfully achieved through Suzuki−Miyaura coupling reaction,[2,8] Mizorogi-Heck coupling reaction,[3−5] and Stille-type coupling reaction.[9] All these reactions consist of oxidative addition of aryl halide to a transition-metal complex, trans-metalation between a metal-aryl complex and an organometallic compound, and reductive elimination, as shown by the mechanism in Scheme 1. Recently, a similar palladium-catalyzed cross-coupling reaction of aryl halide with diboron was reported by Ishiyama, Miyaura, and their collaborators.[10] This reaction receives considerable attention because this is very useful to synthesize a variety of organic boron compounds which are important reagents for organic syntheses. The experimentally proposed mechanism of this reaction consists of the oxidative addition of aryl halide to a palladium(0) complex, the trans-metalation between a palladium(II) aryl complex and diboron, and the reductive elimination. This reaction mechanism is essentially the same as that of Scheme 1. Actually, an interesting common feature was observed in Suzuki−Miyaura coupling reaction and the recently reported palladium-catalyzed cross-coupling reaction of aryl halide with diboron; in both reactions, acceleration by basic condition was reported.[10,11] This accelera-

Scheme 1

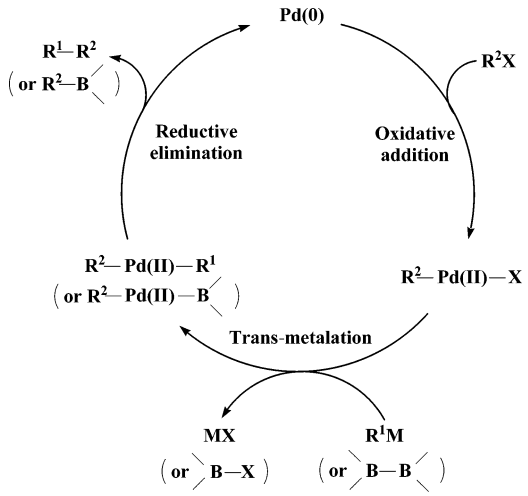

† Department of Molecular Engineering, Graduate School of Engineering, Kyoto University.

‡ Department of Applied Chemistry and Biochemistry, Faculty of Engineering, Kumamoto University.

(1) Trost, B. M. In *Comprehensive Organometallic Chemistry*; Wilkinson, G., Stone, F. G. A., Abel, E. W., Eds.; Pergamon Press. 1982; Vol. 8, 2457.
(2) (a) Miyaura, N.; Suzuki, A. *Chem. Rev.* **1995**, *95*, 2457. (b) Suzuki, A. *J. Organomet. Chem.* **1999**, *576*, 147. (c) Ishiyama, T.; Miyaura, N. *J. Organomet. Chem.* **2000**, *611*, 392.
(3) Crisp, G. T. *Chem. Soc. Rev.* **1998**, *27*, 427.
(4) Stanforth, S. P. *Tetrahedron* **1998**, *54*, 263.
(5) Beletskaya, I. P.; Cheprakov, A. V. *Chem. Rev.* **2000**, *100*, 3009.
(6) Amatore, C.; Jutand, A. *Acc. Chem. Res.* **2000**, *33*, 314.
(7) Whitcombe, N. J.; Hii, K. K.; Gibson, S. E. *Tetrahedron* **2001**, *57*, 7449.
(8) For reviews; (a) Suzuki, A. *Acc. Chem. Res.* **1982**, *15*, 178. (b) Suzuki, A. *Pure Appl. Chem.* **1985**, *57*, 1749. (c) Suzuki, A. *Pure Appl. Chem.* **1991**, *63*, 419. (d) Suzuki, A. *Pure Appl. Chem.* **1994**, *66*, 213.
(9) For reviews; (a) Beletskaya, I. P. *J. Organomet. Chem.* **1983**, *250*, 551. (b) Kosugi, M.; Migita, T. *Yuki Gosei Kyokaishi* (Japanese) **1980**, *38*, 1142, *Chem. Abst.* **1981**, *95*, 81 044d. (c) Stille, J. K. *Angew. Chem., Int. Ed. Engl.* **1986**, *25*, 508.
(10) (a) Ishiyama, T.; Murata, M.; Miyaura, N. *J. Org. Chem.* **1995**, *60*, 7508. (b) Ishiyama, T.; Ahiko, T.; Miyaura, N. *Tetrahedron Lett.* **1996**, 6889. (c) Ishiyama, T.; Itoh, Y.; Kitano, T.; Miyaura, N. *Tetrahedron Lett.* **1997**, 3447. (d) Ahiko, T.; Ishiyama, T.; Miyaura, N. *Chem. Lett.* **1997**, 811.

tion was experimentally interpreted in terms that substitution of halide anion for Lewis base such as OAc^- and OR^- occurred before the trans-metalation under the basic conditions to afford palladium(0)−acetate and −alkoxo complexes, respectively, and the trans-metalation easily proceeds in these complexes.[2a] However, no direct evidence has been presented yet.

Of the elementary processes involved in the catalytic cycle of cross-coupling reaction, the oxidative addition and the reductive elimination have been well investigated theoretically,[12−24] but the trans-metalation process has not been theoretically investigated yet, to our knowledge. In this regard, theoretical study should be performed to clarify the electronic process of the trans-metalation and to understand well the cross-coupling reaction.

In this work, we theoretically investigated the trans-metalation process involved in the palladium-catalyzed borylation of aryl halide with diboron, considering several reasons, as follows: (1) There remain many issues to be elucidated in the trans-metalation, as mentioned above. And, (2) the reaction of transition-metal complexes with boryl compounds exhibits interesting and characteristic features, which are different from those of the reactions with hydride, alkyl, silyl groups, etc., because the boryl group has an empty p_π orbital perpendicular to the molecular plane unlike hydride, alkyl, and silyl groups, as has been experimentally and theoretically reported.[25−30] Such characteristic features of the boryl group are expected to play a key role in the trans-metalation, which would be one of the important reasons of the successful results of this cross-coupling reaction and Suzuki-Miyaura coupling reaction. Our purposes here are to clarify the electronic process of the trans-metalation, to elucidate what is an important factor to accelerate the trans-metalation, and to present useful prediction for further development of this cross-coupling reaction.

Computations and Models

Geometries were optimized with the DFT method, where the B3LYP functional was used for exchange-correlation term.[31,32] Transition states were ascertained by performing frequency calculations and examining geometry changes that are going to occur in each specific imaginary frequency (see Figures S1−S4).

Two kinds of basis set systems were used. The smaller system (BS−I) was employed in geometry optimization. In this BS−I, core electrons (up to 4f) of the Pd atom were replaced with effective core potentials (ECPs) and its valence electrons were represented with a (341/321/31) set.[33] For P, Cl, and I atoms, (21/21/1) sets were used to represent their valence electrons,[34,35] where their core electrons were replaced with ECPs. For B, O, and C atoms, 6-31G(d) sets were employed,[36] whereas the d polarization function was excluded from the basis set for the C atoms of diboron and the boryl group. The better basis set system (BS−II) was employed in evaluation of energy and population changes. In BS−II, a larger (541/541/211) set[33,37] was used for the Pd atom with the same ECPs as those of BS−I. For the B, O, and C atoms, 6-311G(d) sets were employed,[38] whereas the d polarization function was excluded from the C atoms of diboron and the boryl group. The same basis sets and ECPs as those of BS−I were used for the Cl, P, and I atoms.

As will be shown below, the elementary process which involves adduct formation between the palladium complex and diboron will be compared with the process which involves dissociation of phosphine from the palladium complex. In such comparison, entropy effects should be taken into consideration. We evaluated entropy in two ways. In one way, translation, rotation, and vibration movements were considered to estimate entropy, where all substrates were treated as ideal gas. The DFT/BS-I method was adopted to calculate vibration frequencies without scaling factor. In the other way, vibration movements were considered to estimate entropy but translation and rotation movements were not considered, since this reaction was carried out in solution in

(11) (a) Miyaura, N. *J. Organomet. Chem.* **2002**, *653*, 54. (b) Miyaura, N.; Takagi, T.; Suzuki, A. *Synth. Commun.* **1981**, *11*, 513. (c) Watanabe, T.; Miyaura, N.; Suzuki, A. S*ynlett.* **1992**, 207. (d) Satoh, N.; Ishiyama, T.; Miyaura, N.; Suzuki, A. *Bull. Chem. Soc. Jpn.* **1987**, *60*, 3471. (e) Miyaura, N.; Yamabe, K.; Suzuki, A. *Tetrahedron Lett.* **1979**, *20*, 3437.
(12) Saillard, J.-Y.; Hoffmann, R. *J. Am. Chem. Soc.* **1984**, *106*, 2006.
(13) (a) Obara, S.; Kitaura, K.; Morokuma, K. *J. Am. Chem. Soc.* **1984**, *106*, 7482. (b) Koga, N.; Morokuma, K. *J. Am. Chem. Soc.* **1990**, *94*, 7482. (c) Koga, N.; Morokuma, K. *J. Am. Chem. Soc.* **1993**, *115*, 6883. (d) Matsubara, T.; Koga, N.; Musaev, D. G.; Morokuma, K. *J. Am. Chem. Soc.* **1998**, *120*, 12 692.
(14) (a) Low, J. J.; Goddard, W. A. *J. Am. Chem. Soc.* **1986**, *108*, 6115. (b) Low, J. J.; Goddard, W. A. *Organometallics* **1986**, *5*, 609. (c) Xu, X.; Kua, J.; Periana, R. A.; Goddard, W. A. *Organometallics* **2003**, *22*, 2057.
(15) (a) Blomberg, M. R. A.; Siegbahn, P. E. M.; Nagashima, U.; Wennerberg, J. J. *J. Am. Chem. Soc.* **1991**, *113*, 424. (b) Svensson, M.; Blomberg, M. R. A.; Siegbahn, P. E. M. *J. Am. Chem. Soc.* **1991**, *113*, 7076. (c) Blomberg, M. R. A.; Siegbahn, P. E. M.; Svensson, M. *J. Am. Chem. Soc.* **1992**, *114*, 6095. (d) Siegbahn, P. E. M.; Blomberg, M. R. A.; Svensson, M. *J. Am. Chem. Soc.* **1993**, *115*, 4191. (e) Blomberg, M. R. A.; Siegbahn, P. E. M.; Svensson, M. *J. Phys. Chem.* **1994**, *98*, 2062. (f) Siegbahn, P. E. M.; Blomberg, M. R. A. *Organometallics* **1994**, *13*, 354. (g) Siegbahn, P. E. M. *Organometallics* **1994**, *13*, 2833. (h) Siegbahn, P. E. M.; Svensson, M. *J. Am. Chem. Soc.* **1994**, *116*, 10 124. (i) Siegbahn, P. E. M. *J. Am. Chem. Soc.* **1996**, *118*, 1487. (j) Siegbahn, P. E. M.; Crabtree, R. H. *J. Am. Chem. Soc.* **1996**, *118*, 4442.
(16) (a) Song, J.; Hall, M. B. *Organometallics* **1993** *12*, 3118. (b) Jimenez-Catao, R.; Hall, M. B. *Organometallics* **1996**, *15*, 1889. (c) Niu, S. -Q.; Hall, M. B. *J. Am. Chem. Soc.* **1998**, *120*, 6169.
(17) (a) Sakaki, S.; Ieki, M. *J. Am. Chem. Soc.* **1993**, *115*, 2373. (b) Sakaki, S.; Biswas, B.; Sugimoto, M. *J. Chem. Soc., Dalton Trans.* **1997**, 803. (c) Sakaki, S.; Biswas, B.; Sugimoto, M. *Organometallics* **1998** *17*, 1278. (d) Sakaki, S.; Mizoe, N.; Musashi, Y.; Biswas, B.; Sugimoto, M. *J. Phys. Chem.* **1998**, *41*, 8027. (e) Sakaki, S.; Kai, S.; Sugimoto, M. *Organometallics* **1999** *18*, 4825.
(18) Hinderling, C.; Feichtinger, D.; Plattner, D. A.; Chen, P. *J. Am. Chem. Soc.* **1997**, *119*, 10 793.
(19) Su, M.-D.; Chu, S.-Y. *J. Am. Chem. Soc.* **1997**, *119*, 5373.
(20) Espinosa-Garcia, J.; Corchando, J. C.; Truhlar, D. G. *J. Am. Chem. Soc.* **1997**, *119*, 9891.
(21) Hill, G. S.; Puddephatt, R. J. *Organometallics* **1998** *17*, 1478.
(22) Bartlett, K. L.; Goldberg, K. I.; Borden, W. T. *Organometallics* **2001** *20*, 2669.
(23) Gilbert, T. M.; Hristov, I.; Ziegler, T. *Organometallics*, **2001**, *20*, 1183.
(24) Ustymyuk, Y. A.; Ustynyuk, L. Y.; Laikov, D. N.; Lunin, V. V. *J. Organomet. Chem.* **2000**, *597*, 182.
(25) For recent reviews: (a) Hartwig, J. F.; Waltz, K. M.; Muhoro, C. N.; He, X.; Eisenstein, O.; Bosque, R.; Maseras, F., In *Advances of Boron Chemistry*, Siebert, W., Ed.; Spec. Publ. No. 201, Royal Society of Chemistry: Cambridge, U. K., 1997; p373. (b) Wadepohl, H. *Angew. Chem., Int. Ed. Engl.* **1997**, *36*, 2441. (c) Irvine, G. J.; Lesley, M. J. G.; Marder, T. B.; Norman, N. C.; Rice, C. R.; Robins, E. G.; Roper, W. R.; Whittell, G. R.; Wright, L. J. *Chem. Rev.* **1998**, *98*, 2685. (d) Braunschweig, H. *Angew. Chem., Int. Ed. Engl.* **1998**, *37*, 567. (e) Smith, R. M. III. *Prog. Inorg. Chem.* **1999**, *48*, 505. (f) Braunschweig, H.; Colling, M. *Coord. Chem. Rev.* **2001**, *223*, 1. (g) Huang, X.; Lin, Z. Y. In *Computational Modeling of Homogeneous Catalysis*, Maseras, F.; LLedos, A., Eds.; Kluwer Academic: Amsterdam, 2003; p189.
(26) (a) Uddin, J.; Frenking, G. *J. Am. Chem. Soc.* **2001**, *123*, 1683. (b) Chen, Y.; Frenking, G. *J. Chem. Soc., Dalton Trans.* **2001**, 434.
(27) (a) Cui, Q.; Musaev, D. G.; Morokuma, K. *Organometallics*, **1998**, *17*, 742. (b) Cui, Q.; Musaev, D. G.; Morokuma, K. *Organometallics* **1997**, *16*, 1355.
(28) (a) Sakaki, S.; Kikuno, T. *Inorg. Chem.* **1997**, *36*, 226. (b) Sakaki, S.; Kai, S.; Sugimoto, M. *Organometallics* **1999**, *18*, 4825. (c) Tamura, H.; Yamasaki, H.; Sato, H.; Sakaki, S. *J. Am. Chem. Soc.* **2003**, *125*, 16 114.
(29) Widauer, C.; Grützmacher, H.; Ziegler, T. *Organometallics* **2000**, *19*, 2097.
(30) (a) Han, W. H.; Lin, Z. *Organometallics* **2000**, *19*, 2625. (b) Liu, D.; Lin, Z. *Organometallics* **2002**, *21*, 4750. (c) Lam, W. H.; Lin, Z. *Organometallics* **2003**, *22*, 473. (d) Liu, D.; Lam, K. C.; Lin, Z. *Organometallics* **2003**, *22*, 2827.
(31) Becke, A. D. *Phys. Rev. A*, **1988**, *38*, 3098. (b) Becke, A. D. *J. Chem. Phys.* **1983**, *98*, 5648.
(32) Lee, C.; Yang, W.; Parr, R. G. *Phys. Rev. B*, **1988**, *37*, 785.
(33) Hay, P. J.; Wadt, W. R. *J. Chem. Phys.* **1985**, *82*, 299.
(34) Wadt, W. R.; Hay, P. J. *J. Chem. Phys.* **1985**, *82*, 284.
(35) Höllwarth, A.; Böhme, M.; Dapprich, S.; Ehlers, A. W.; Gobbi, A.; Jonas, V.; Köhler, K. F.; Stegmann, R.; Veldkamp, A.; Frenking, G. *Chem. Phys. Lett.*, **1993**, *208*, 237.
(36) (a) Ditchfiled, R.; Hehre, W. J.; Pople, J. A. *J. Chem. Phys.* **1971**, *54*, 724. (b) Hariharan, P. C.; Pople, J. A. *Mol. Phys.* **1974**, *27*, 209.
(37) Couty, M.; Hall, M. B. *J. Comput. Chem.* **1996**, *17*, 1359.
(38) Krishnan, R.; Binkley, J. S.; Seeger, R.; Pople, J. A. *J. Chem. Phys.* **1980**, *72*, 650.

Scheme 2

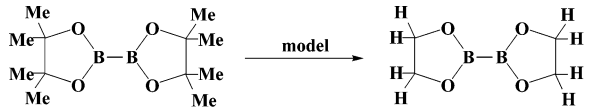

Bis(pinacolato)diboron **Bis(ethyleneglycolato)diboron**

which the translation and rotation movements are highly suppressed. The free energy change estimated in this way is named ΔG_v^0 hereafter. In the former method, entropy significantly decreases when two molecules form an adduct, as expected. The latter method, on the other hand, provides much smaller entropy change than does the former method, as will be discussed below. The former method apparently overestimates the entropy effects and the thermal energy of solution reaction, because translation and rotation movements are highly suppressed in solution. On the other hand, the latter one underestimates the entropy effects and the thermal energy because translation and rotation movements are not completely suppressed in solution.[39] The true value of free energy change would be intermediate between the $\Delta G°$ value by the former method and the ΔG_v^0 value by the latter one, and more or less close to the ΔG_v^0 value estimated by the latter method in the solution reaction. Because this ambiguity remains in estimation of entropy and thermal energy, we will discuss each elementary step with the usual potential energy changes and then discuss it with the free energy changes evaluated in two ways.

Gaussian 98 program package was used for all calculations.[40] Population analysis was carried out with the method proposed by Weinhold et al.[41] Solvent effects were incorporated in some of reactions with the PCM method.[42] Contour map of molecular orbital was drawn with Molden program package.[43]

Bis(pinacolato)diboron, $B_2(pin)_2$ (pin = $-OCMe_2CMe_2O-$), that was experimentally used,[10] was modeled here with bis(ethyleneglycolato)-diboron, $B_2(eg)_2$ (eg = $-OCH_2CH_2O-$), as shown in Scheme 2, like our previous work.[28c] In Suzuki−Miyaura coupling reaction and the palladium-catalyzed borylation of halobenzene with diboron, formation of the palladium(II) hydroxo complex was experimentally proposed under basic conditions (vide supra).[2a,44,45] Actually, palladium(II) hydroxo and similar palladium(II) alkoxo complexes have been reported, so far.[46−49] Moreover, a palladium(II) methoxo vinyl complex undergoes the cross-coupling reaction with organic boron ester.[44] Considering the experimental proposal and the experimental results, we investigated the trans-metalation of palladium(II) hydroxo phenyl complex, Pd(Ph)-(OH)$(PH_3)_2$, with diboron, $B_2(eg)_2$. In the trans-metalation, we examined two possible reaction courses, as shown in Scheme 3; one is associative substitution of PH_3 for $B_2(eg)_2$ followed by the trans-metalation. Coordination of $B_2(eg)_2$ with the Pd center is not surprising because $B_2(eg)_2$ has a lone pair orbital on the O atom.[50] Actually, the coordination of diboron with the metal center has been theoretically reported.[27,28c] The other one is dissociative substitution of PH_3 for B_2-$(eg)_2$ followed by the trans-metalation, in which there are two isomers of Pd(OH)(Ph)(PH_3), as shown in Scheme 3. The alternative explanation of the base effects was proposed in the experimental field; it was based on the idea that not diboron but [diboron−OH]$^-$ adduct reacted with the palladium(II) phenyl complex.[2c] The formation of diboron adduct with Lewis base provides experimental support to the formation of the [diboron−OH]$^-$ adduct.[51,52] Although this explanation is also worthy of investigation, the trans-metalation process investigated here is considered to be essentially the same as the reaction of [diboron−OH]$^-$ with the palladium(II) phenyl complex, as will be described below.

Results and Discussion

Model of Active Species. The first step of the palladium-catalyzed borylation of aryl halide with diboron is believed to be oxidative addition of aryl halide to a palladium(0) complex (see Scheme 1). When the oxidative addition to Pd$(PH_3)_2$ **1** proceeds via a concerted transition state, the product is *cis*-Pd-(I)(Ph)$(PH_3)_2$ **2** in which I and Ph ligands take positions cis to each other. When the oxidative addition proceeds with dissociation of halide anion, **2** and/or the trans-isomer **3** are produced as a product. The trans-form is more stable than the cis-form by about 5 kcal/mol (see Supporting Information Figure S-5). The cis-trans isomerization is accelerated by the presence of Lewis base, in general. Because OH^- would play a role of Lewis base, this isomerization easily occurs under basic conditions. Also, it was reported experimentally that the substitution of I^- for OH^- easily took place in the basic solvent.[2a,53] Actually, *trans*-Pd(OH)(Ph)$(PH_3)_2$ **4** is much more stable than **3** (Supporting Information Figure S-5). Thus, it is likely to consider that **4** is an active species.

Geometry Changes in Associative Substitution of PH_3 Followed by Trans-metalation. We will first investigate the associative substitution of PH_3 for $B_2(eg)_2$ followed by the trans-metalation (See Scheme 3). $B_2(eg)_2$ approaches *trans*-Pd(OH)-(Ph)$(PH_3)_2$ **4**, to afford a reactant complex, *trans*-Pd(OH)(Ph)-$(PH_3)_2[B_2(eg)_2]$ **5**, as shown in Figure 1. In **5**, $B_2(eg)_2$ does not

(39) (a) These two ways to estimate the entropy were adopted in our previous works.[28c, 39b] (b) Sakaki, S.; Takayama, T.; Sumimoto, M.; Sugimoto, M. *J. Am. Chem. Soc.*, **2004**, *126*, 3332.

(40) Frisch, M. J.; Trucks, G. W.; Schlegel, H. B.; Scuseria, G. E.; Robb, M. A.; Cheeseman, J. R.; Zakrzewski, V. G.; Montgomery, J. A.; Stratmann, R. E.; Burant, J. C.; Dapprich, S.; Millam, J. M.; Daniels, A. D.; Kudin, K. N.; Strain, M. C.; Farkas, O.; Tomasi, J.; Barone, V.; Cossi, M.; Cammi, R.; Mennucci, B.; Pomelli, C.; Adamo, C.; Clifford, S.; Ochterski, J.; Petersson, G. A.; Ayala, P. Y.; Cui, Q.; Morokuma, K.; Malick, D. K.; Rabuck, A. D.; Raghavachari, K.; Foresman, J. B.; Cioslowski, J.; Ortiz, J. V.; Stefanov, B. B.; Liu, G.; Liashenko, A.; Piskorz, P.; Komaromi, I.; Gomperts, R.; Martin, R. L.; Fox, D. J.; Keith, T.; Al-Laham, M. A.; Peng, C. Y.; Nanayakkara, A.; Gonzalez, C.; Challacombe, M.; Gill, P. M. W.; Johnson, B. G.; Chen, W.; Wong, M. W.; Andres, J. L.; Head-Gordon, M.; Replogle, E. S.; Pople, J. A. *Gaussian 98*, Gaussian Inc., Pittsburgh, PA, **1998**.

(41) Reed, A. E.; Curtis, L. A.; Weinhold, F. *Chem. Rev.* **1988**, *88*, 849, and references therein.

(42) (a) Miertus, S.; Scrocco, E.; Tomasi, J. *Chem. Phys.* **1981**, *55*, 117. (b) Miertus, S.; Tomasi, J. *Chem. Phys.* **1982**, *65*, 239. (c) Cossi, M.; Barone, V.; Cammi, R.; Tomasi, J. *Chem. Phys. Lett.* **1996**, *255*, 327.

(43) Schaftenaar, G.; Noordik, J. H. *J. Comput. -Aided Mol. Des.* **2000**, *14*, 123.

(44) (a) Miyaura, N.; Yamada, K.; Suginome, M.; Suzuki, A. *J. Am. Chem. Soc.* **1985**, *107*, 972. (b) Satoh, N.; Ishiyama, T.; Miyaura, N.; Suzuki, A. *Bull. Chem. Soc. Jpn.* **1987**, *60*, 3471.

(45) Mandai, T.; Suzuki, S. Ikawa, A.; Murakami, T.; Kawada, M. Tsuji, J. *Tetrahedron Lett.* **1991**, *32*, 7687.

(46) Yoshida, T.; Okano, T.; Otsuka, S. *J. Chem. Soc., Dalton Trans.* **1976**, 993.

(47) (a) Tsuji, J.; Watanabe, H.; Minami, I.; Shimizu, I. *J. Am. Chem. Soc.* **1985**, *107*, 2196. (b) Minami, I.; Yuhara, Y.; Watanabe, H.; Tsuji, J. *J. Organomet. Chem.* **1987**, *234*, 225. (c) Tsuji, J.; Sugiura, T.; Minami, I. *Tetrahedron Lett.* **1986**, *27*, 731. (d) Tsuji, J.; Sugiura, T.; Yuhara, M.; Minami, I. *J. Chem. Soc., Dalton Trans.* **1986**, 922. (e) Mandai, T.; Ogawa, M.; Yamaoki, H.; Nakata, T.; Murayama, H.; Kawada, M.; Tsuji, J. *Tetrahedron Lett.* **1991**, *32*, 3397.

(48) Siegmann, K.; Pregosin, P. S.; Venanzi, L. M. *Organometallics* **1989**, *8*, 2659.

(49) Grushin, V. V.; Alper, H. *Organometallics* **1993**, *12*, 1890.

(50) Four methyl groups of $B_2(pin)_2$ are substituted for four H atoms in B_2-$(eg)_2$. This suggests that $B_2(eg)_2$ more strongly interacts with the Pd center and the OH ligand than does $B_2(pin)_2$ because of the smaller steric repulsion. Thus, the Pd−Beg and X−Beg interactions would be overestimated in the present study, to some extent.

(51) Such base as pyridine forms an adduct with bis(catecholato)diboron, B_2-$(cat)_2$, but does not form an adduct with $B_2(pin)_2$.[52] In the palladium-catalyzed borylation of halobenzene with diboron, however, we cannot completely neglect the possibility that $B_2(pin)_2$ forms an adduct with OH^- and OR^- because these bases are much stronger and much less bulky than pyridine.

(52) (a) Nguyen, P.; Dai, C.; Taylor, N. J.; Power, W. P.; Marder, T. B.; Pickett, N. L.; Norman, N. C. *Inorg. Chem.* **1995**, *34*, 4290. (b) Clegg, W.; Dai, C.; Lawlor, F. J.; Marder, T. B.; Nguyen, P.; Norman, N. C.; Pickett., N. L. Power, W. P.; Scott, A. *J. Chem. Soc., Dalton Trans.* **1997**, 839. (c) Clegg, W.; Scott, A. J.; Souza, F. E. S.; Marder, T. B. *Acta Crystallogr.* **1999**, *C55*, 1885.

(53) Maitlis, P. M. *The Organic Chemistry of Palladium*; Academic: New York, 1971; vol.2, pp 119−120.

Scheme 3

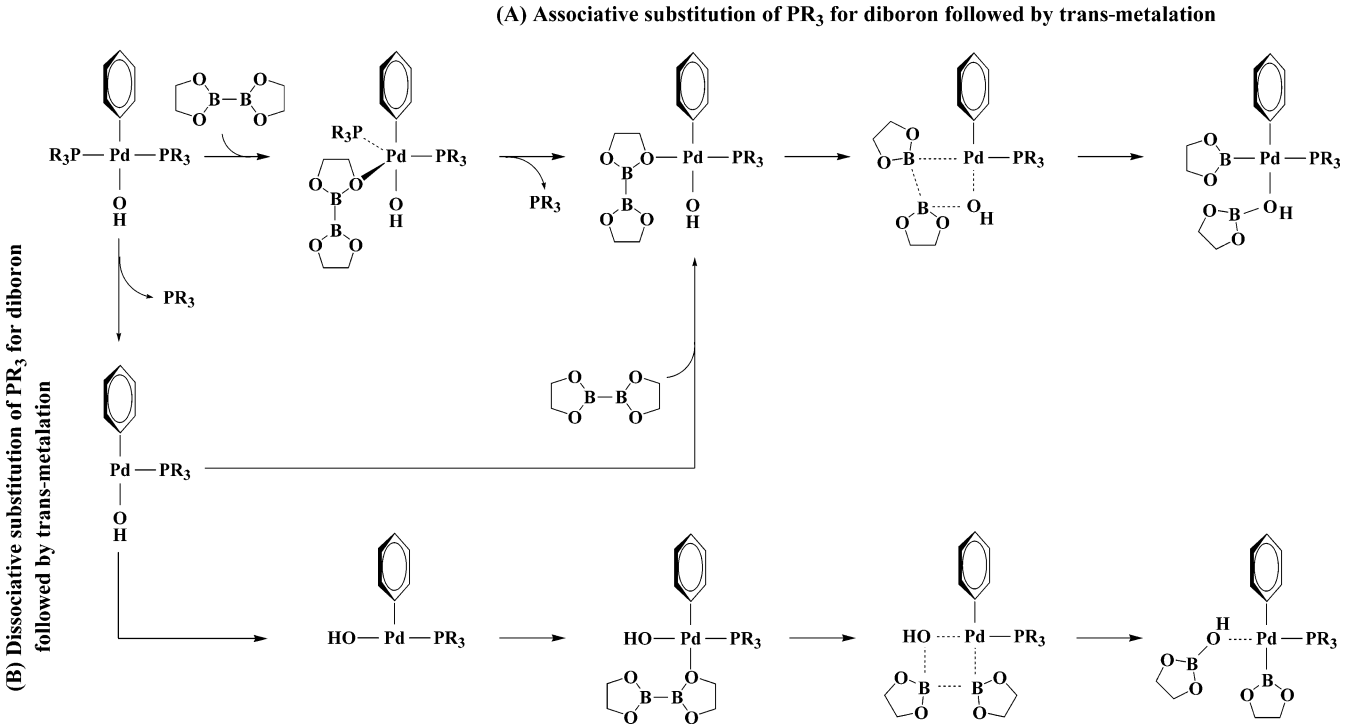

interact with the Pd center but interacts with the OH ligand, in which the B−O distance is 1.533 Å.[55] This interaction arises from the charge-transfer from the lone pair orbital of the OH ligand to the empty p orbital of the Beg[a] group, as will be discussed in terms of population changes below (see Figure 1 for Beg[a] and Beg[b]). On the other hand, the Beg[b] group is distant from the Pd center; see the distance of 3.365 Å between the Pd center and the O[boryl] atom of $B_2(eg)_2$, where the O[boryl] atom represents the O atom of the Beg[b] group, hereafter. Complex **5** udnergoes the dissociation of PH_3[a] from the Pd center, to afford a four-coordinate complex, *trans*-Pd(OH)(Ph)(PH_3)[$B_2(eg)_2$] **6**, through the transition state $\mathbf{TS_{5-6}}$. This transition state $\mathbf{TS_{5-6}}$ takes a typical trigonal bipyramidal structure, in which the O[boryl] atom of the Beg[b] group is approaching the Pd center to push one PH_3[a] away from the Pd center. The distance between the Pd center and the O[boryl] atom becomes considerably shorter,

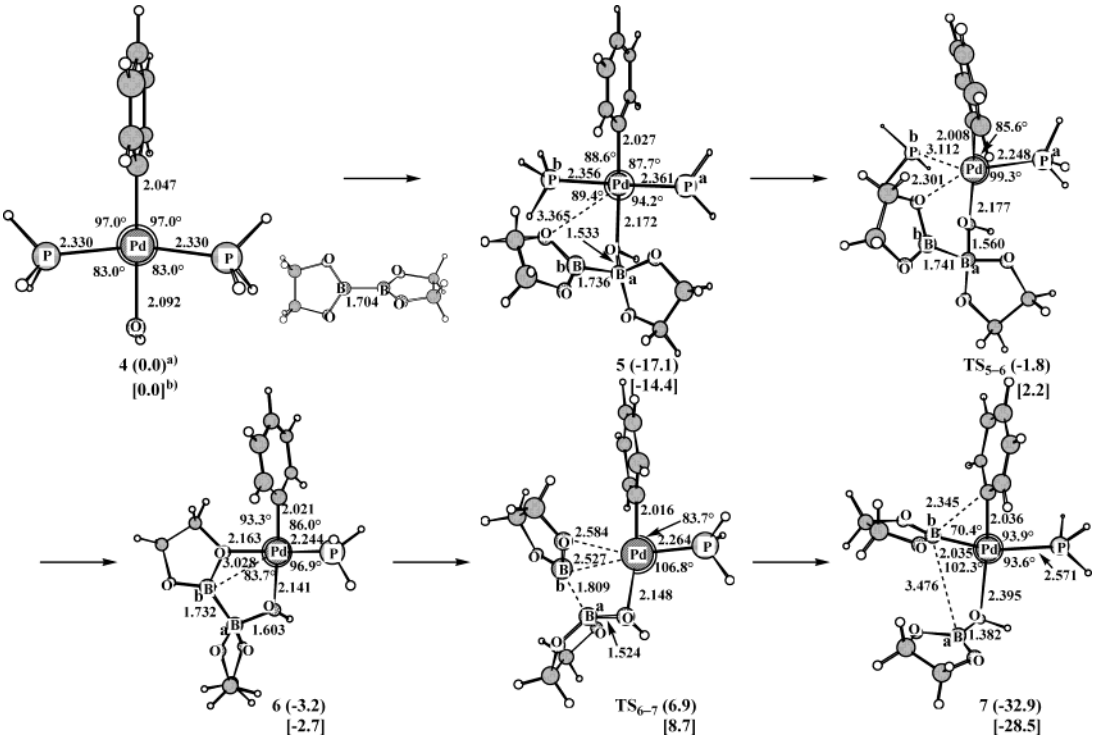

Figure 1. Geometry and energy changes by associative substitution of PH_3 for diboron, $B_2(eg)_2$, followed by trans-metalation in Pd(OH)(Ph)(PH_3)$_2$. Bond lengths are in Å and bond angles in degrees. (a) Relative energies (kcal/mol) to the sums of reactants, in which the DFT/BS-II method was used, are in parentheses. (b) Relative energies in diethyl ether, in which the DFT/BS-II method was used with the PCM method, are in brackets (kcal/mol).

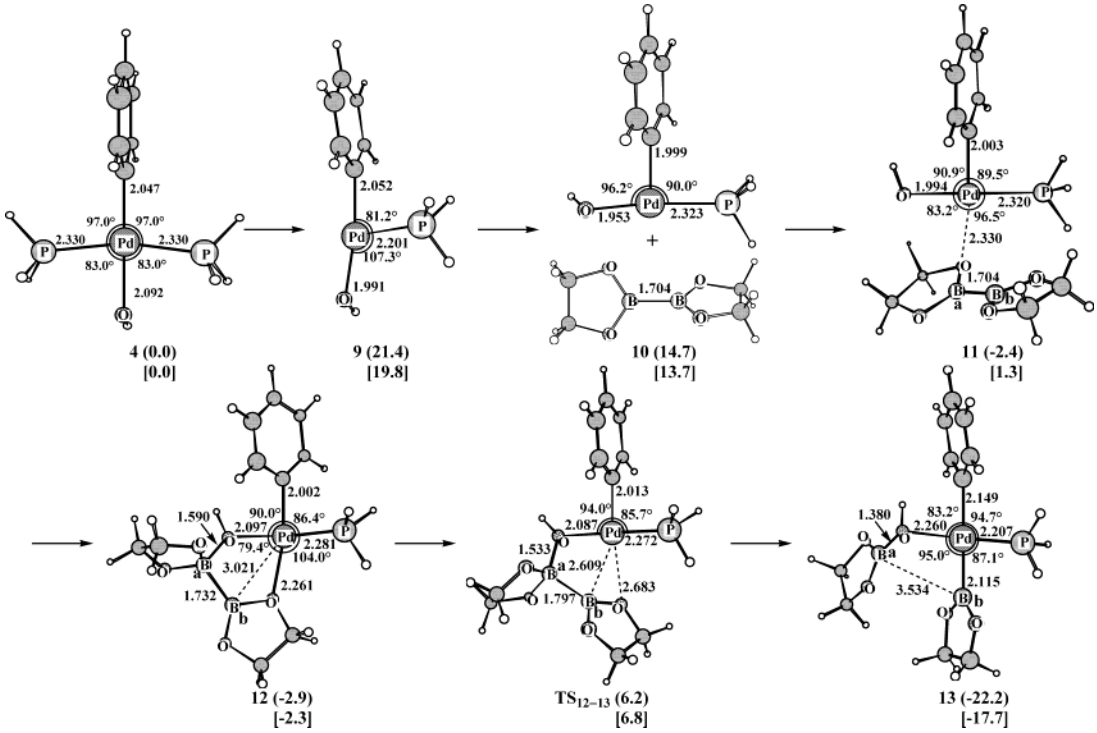

Figure 2. Geometry and energy changes by dissociative substitution of PH_3 for diboron, $B_2(eg)_2$, followed by trans-metalation in $Pd(OH)(Ph)(PH_3)_2$. Bond lengths are in Å and bond angles are in degrees. (a) Relative energies (kcal/mol) to the sum of reactants, in which the DFT/BS-II method was used, are in parentheses. (b) Relative energies in diethyl ether, in which the DFT/BS-II method was used with the PCM method, are in brackets (kcal/mol).

which indicates that the coordinate bond of the Beg^b group with the Pd center has been almost formed in the transition state. Consistent with the rather short $Pd-O^{boryl}$ distance, the $Pd-PH_3{}^a$ distance considerably lengthens to 3.112 Å. This long distance indicates that the $PH_3{}^a$ ligand little interacts with the Pd center in $\mathbf{TS_{5-6}}$. Complex **6** takes a typical four-coordinate planar structure, in which the Pd−OH distance (2.163Å) is similar to the usual coordinate bond distance of the OH ligand. This Pd−OH distance indicates that the OH group still coordinates well with the Pd center after formation of the bonding interaction between OH and Beg^a groups. Such coordination of HO−Beg is not surprising because the OH group has two lone pair orbitals on the O atom; one is used for the interaction with the Pd center and the other is used for the interaction with the Beg^a group. From **6**, the B−B bond scission proceeds through the transition state $\mathbf{TS_{6-7}}$, leading to $Pd(Beg^b)(Ph)(PH_3)(HO-Beg^a)$ **7**. In $\mathbf{TS_{6-7}}$, the Beg^b group, which will be bound with the Pd center in **7**, is changing its direction toward the Pd center and the $Pd-O^{boryl}$ distance becomes longer than that of **6**. The B−B and Pd−OH distances become somewhat longer and the HO−Beg^a distance becomes shorter. All of these geometry changes show that the B−B bond scission, the HO−Beg^a bond strengthening, the Pd−OH bond weakening, and the $Pd-O^{boryl}$ bond scission are in progress in $\mathbf{TS_{6-7}}$. Complex **7** takes a typical four-coordinate planar structure, in which the Pd−Beg^b bond is formed. Also, the HO−Beg^a group still coordinates well with the Pd center in **7**.

It is noted here that **5** is understood in terms of the palladium complex with the [diboron-OH]$^-$ adduct. Thus, the trans-metalation occurs in a similar manner if the [diboron-OH]$^-$ adduct is formed under the basic condition.

Geometry Changes in Dissociative Substitution of PH_3 Followed by Trans-metalation. A three-coordinate complex, *trans*-Pd(OH)(Ph)(PH_3) **9**, is formed from *trans*-Pd(OH)(Ph)-$(PH_3)_2$ **4**, through dissociation of PH_3 from the Pd center. In **9**, the OH ligand is at a position trans to the Ph ligand, as shown in Figure 2. Complex **9** is much less stable than **4** by 21.4 kcal/mol. However, **9** easily isomerizes to *cis*-Pd(OH)(Ph)(PH_3) **10** with a very small barrier of 1.2 kcal/mol.[54a] Complex **10** is less stable than **4** by 14.7 kcal/mol. Since **10** has one vacant site at a position trans to the Ph ligand, $B_2(eg)_2$ easily approaches this vacant site, to afford *cis*-Pd(OH)(Ph)(PH_3)[$B_2(eg)_2$] **11**. In **11**, $B_2(eg)_2$ coordinates with the Pd center through the O atom like **6**.[50] However, **11** is not the most stable, but **12** is slightly more stable than **11** by 0.5 kcal/mol.[54b] In **12**, the Beg^a group interacts with the OH ligand. In this structure, the unoccupied p orbital of the Beg^a group interacts with the lone pair orbital of the OH ligand like that of **5**. The B−O distance between the Beg^a group and the OH ligand is 1.590 Å which is moderately longer than that of hydroxyborane, HO−Beg, by about 0.2 Å. Because of this bonding interaction, the Pd−OH bond becomes longer by ca. 0.1 Å, which then strengthens the $Pd-PH_3$ bond; actually, this $Pd-PH_3$ bond becomes shorter by ca. 0.04 Å. Complex **12** undergoes the B−B bond scission, to afford Pd(Ph)(Beg^b)(PH_3)-

(54) (a) Since the dissociative substitution followed by the trans-metalation is less favorable than the associative substitution followed by the trans-metalation, as described in the text, the reaction course involving the dissociative substitution is not investigated in detail here. Thus, we roughly estimated the activation barrier by calculating the energy change as a function of the X−Pd−P angle (X = HO, F, or Cl). (b) Because of the above reason, we did not optimize the transition state of this process.

(55) (a) Because the bulky phosphine such as *t*-buthylphosphine more easily dissociates from the Pd center than small phosphine, the dissociative substitution would occurs easier in the real reaction system than in the model system of PH_3. However, the coordination of diboron would become difficult in such Pd complex of bulky phosphine. This means that compensation would occur upon going from PH_3 complexes to real phosphine complexes. (b) The solvent molecule stabilizes the coordinatively unsaturated intermediate through the coordination. However, the dissociation of phosphine must occur first in the dissociative substitution. Thus, it is likely to consider that the rate-determining step is dissociation of phosphine.

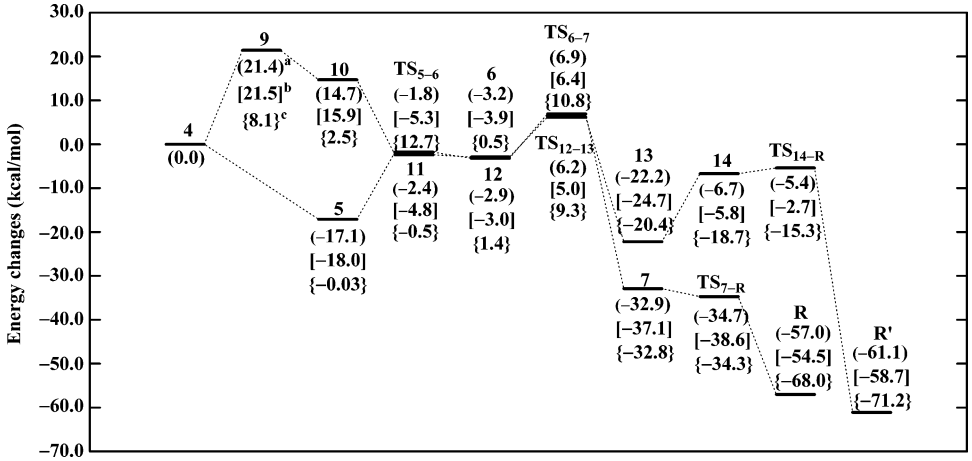

Figure 3. Energy changes in associative substitution of PH_3 for $B_2(eg)_2$ followed by trans-metalation and dissociative substitution followed by trans-metalation of $Pd(OH)(Ph)(PH_3)_2$. The DFT/BS-II method; kcal/mol unit. (a) Potential energy changes. (b) Gibbs free energy changes (ΔG_v^0) at 298 K, where only vibration movements are taken into consideration in the estimation of free energy. (c) Gibbs free energy changes ($\Delta G°$) at 298 K in gas-phase reaction, where translation, rotation, and vibration movements are taken into consideration in the estimation of free energy.

(HO−Beg[a]) **13** through transition state **TS$_{12-13}$**. In **TS$_{12-13}$**, the Beg[b] group is changing its direction toward the Pd center and the Beg[a] group is changing its direction toward the OH ligand. However, the B−B distance does not become very longer, and the geometry of the other moiety also little changes. In the product **13**, HO−Beg strongly coordinates with the Pd center like that of **7**, where the Pd−OH distance is 2.260 Å.

Energy Changes in the Substitution of PH_3 for $B_2(eg)_2$ followed by the Trans-metalation. Potential energy changes along the associative substitution followed by the trans-metalation are shown in Figure 3 (see the values in parentheses). Apparently, the interaction of $B_2(eg)_2$ with the OH ligand yields a considerably large stabilization energy of 17.1 kcal/mol in **5**.[50] Complex **5** undergoes the substitution of PH_3 for the Beg[b] group with a moderate activation barrier of 15.5 kcal/mol, to afford **6**. The intermediate **6** is slightly more stable than **TS$_{5-6}$** by only 1.4 kcal/mol and the transition state **TS$_{6-7}$** is less stable than **6** by 10.1 kcal/mol. Thus, the energy difference of 24.0 kcal/mol between **TS$_{6-7}$** and **5** should be taken as the activation barrier (E_a) of the reaction from **5** to **7**, because the reverse reaction from **6** to **5** easily takes place with a much smaller E_a value of 1.4 kcal/mol than that (10.1 kcal/mol) of the forward reaction from **6** to **7**. The other important result is that the exothermicity of this trans-metalation is significantly large; 32.9 kcal/mol relative to **4** and 15.8 kcal/mol relative to **5**. From these results, it is concluded that the associative substitution followed by the trans-metalation takes place with a moderate E_a value of 24.0 kcal/mol.

The energy changes along the trans-metalation via the dissociative substitution are also shown in Figure 3. Apparently, the dissociation of PH_3 gives rise to considerably large destabilization energy (21.4 kcal/mol). This destabilization energy is partially recovered by the isomerization of **9** to **10**. Coordination of $B_2(eg)_2$ with **10** yields considerably large stabilization energy of 17.1 kcal/mol.[50] The E_a value of the B−B bond scission is 9.1 kcal/mol and its exo-thermicity is considerably large (32.9 kcal/mol). Thus, the rate-determining step of this dissociative substitution followed by the trans-metalation is the dissociation of PH_3 from the Pd center.[55] Although the E_a value of the B−B bond scission is much smaller than that of the associative substitution followed by the trans-metalation, the dissociation of PH_3 gives rise to significantly large destabilization energy. In the trans-metalation via the associative substitution, on the other hand, $B_2(eg)_2$ approaches the OH ligand to afford the intermediate **5** with considerably large stabilization energy of 17.1 kcal/mol. Because $B_2(eg)_2$ exists in excess under the catalytic reaction conditions, it should be concluded that **4** completely converts to **5**. Although the solvent molecule coordinates with the Pd center of coordinatively unsaturated intermediates **9** and **10** to stabilize them, the phosphine dissociation must occur in the dissociative substitution to afford **9**. This means that **9** corresponds to the transition state in the dissociative substitution. Transition state **TS$_{6-7}$** is at a much lower energy than **9**, where **TS$_{6-7}$** and **9** are at the highest energy in the reaction course via the associative substitution and that via the dissociative one, respectively. These results indicate that the trans-metalation more easily takes place via the associative substitution than that via the dissociative one.

Here, we wish to compare these two reaction courses with free energy changes ($\Delta G°$) at 298 K. As shown in Figure 3, the $\Delta G°$ value of the process from **4** to **9** is much smaller than the potential energy change (see values in braces of Figure 3), where the translation, rotation, and vibration movements are considered in the estimation of the $\Delta G°$ value. This is because the dissociation of PH_3 occurs in the process from **4** to **9**. The next step is the isomerization from **9** to **10**, in which the $\Delta G°$ value is similar to the potential energy change. Upon going to **11** from **10**, the $\Delta G°$ value moderately decreases to −0.5 kcal/mol. This decrease in $\Delta G°$ is much smaller than that of the potential energy change because the adduct formation of $B_2(eg)_2$ with the Pd center occurs in this step. Then, the B−B bond scission takes place in the process from **12** to **13**, which induces the activation free energy change ($\Delta G^{0‡}$) of 7.9 kcal/mol. This value is similar to the E_a value (9.1 kcal/mol) evaluated from the potential energy change. In the reaction course via the associative substitution, on the other hand, the reaction from **4** to **5** induces significantly larger $\Delta G°$ value than the potential energy change, because this process involves the adduct formation of $B_2(eg)_2$ with the Pd center. The activation free energy change ($\Delta G^{0‡}$) of the reaction from **5** to **TS$_{5-6}$** is somewhat smaller than the E_a value; $\Delta G^{0‡} = 12.7$ kcal/mol and $E_a = 15.3$ kcal/mol. This is probably because PH_3 is dissociating

from the Pd center in **TS$_{5-6}$**. The significant difference between potential energy change and free energy change is observed in **6**. In the potential energy change, **6** is only slightly more stable than **TS$_{5-6}$**, whereas it is much more stable than **TS$_{5-6}$** in the free energy change because **6** is formed through PH_3 dissociation from the Pd center. The $\Delta G^{0\ddagger}$ value for the B−B bond scission (**6** → **TS$_{6-7}$**) is 10.3 kcal/mol. Because this $\Delta G^{0\ddagger}$ value (10.3 kcal/mol) for the forward reaction (**6** → **7**) is somewhat smaller than that (12.2 kcal/mol) of the reverse reaction (**6** → **5**), the $\Delta G^{0\ddagger}$ value of the process from **5** to **7** corresponds to the free energy difference between **5** and **TS$_{5-6}$**. Its value (12.7 kcal/mol) is moderately larger than the $\Delta G°$ value of 8.1 kcal/mol for PH_3 dissociation (**4** → **9**). Also, it is noted that **TS$_{5-6}$** is at somewhat higher energy than **9**, where **TS$_{5-6}$** and **9** are at the highest energy in the reaction course via the associative substitution and that via the dissociative one, respectively. Thus, it is concluded that the reaction via the dissociative substitution more easily proceeds than that via the associative one in gas phase.

However, the above $\Delta G°$ values are considerably different from the true $\Delta G°$ value in solution, because the translation and rotation movements are highly suppressed in solution. It is likely to suppose that the ΔG_v^0 value without contribution of translation and rotation movements is more or less close to the true value of the free energy change in solution (see the section of Computations and Models). The ΔG_v^0 value of the process **4** → **9** is 21.5 kcal/mol and that of the process **4** → **5** is −18.0 kcal/mol (see the values in brackets of Figure 3). The difference in free energy change between **5** and **TS$_{5-6}$** should be taken as an activation free energy change ($\Delta G_v^{0\ddagger}$) to reach **7** from **5**, because the $\Delta G_v^{0\ddagger}$ value of the forward reaction from **6** to **7** is much larger than that of the reverse reaction from **6** to **5**. This $\Delta G_v^{0\ddagger}$ value (24.4 kcal/mol) of the process from **5** to **7** is moderately larger than the ΔG_v^0 value (21.5 kcal/mol) for the PH_3 dissociation (**4** → **9**) in the dissociative substitution. However, the ΔG_v^0 value of **TS$_{6-7}$** is much smaller than that of **9** by 15.1 kcal/mol, where **TS$_{6-7}$** and **9** are the most unstable species in the reaction course via the associative substitution and that via dissociative one, respectively. Also, it is noted that **4** completely converts not to **9** but to **5**, since the ΔG_v^0 values indicate that **5** is much more stable than **4** but **9** is much less stable than **4**. From these results, it should be concluded that the associative substitution followed by the trans-metalation takes place more favorably than the dissociative one in solution.

At the end of this section, we wish to mention the solvent effects on these energy changes, where diethyl ether was adopted as a model of dioxane used experimentally.[10] The PCM calculations clearly show that the solvent effects do not alter energy changes very much, as shown in brackets of Figures 1 and 2. Solvent effects were not considered hereafter.

Electronic Processes in the B−B Bond Scission. In Pd(OH)(Ph)$(PH_3)_2[B_2(eg)_2]$ **5**, the electron population of OH considerably decreases and that of Beg^a considerably increases, as shown in Table 1 (see Figure 1 for Beg^a etc.). These are because the charge-transfer occurs from OH to the empty p orbital of Beg^a. In **TS$_{5-6}$**, the electron population of $PH_3{}^b$ considerably increases and the Pd atomic population considerably decreases, because $PH_3{}^b$ little interacts with the Pd center and the charge-transfer from $PH_3{}^b$ to the Pd center becomes very weak in this transition state. On the other hand, the electron population of Beg^b somewhat decreases, because Beg^b starts to form the charge-transfer interaction with the Pd center in **TS$_{5-6}$**.

Table 1. Population Changes[a] in the Trans-metalation Process

(A) trans-metalation of Pd(OH)(Ph)$(PH_3)_2$ via associative substitution of PH_3 for $B_2(eg)_2$

	4	**5**	**TS$_{5-6}$**	**6**	**TS$_{6-7}$**	**7**
Pd	0.0	−0.017	−0.228	−0.187	−0.166	−0.148
OH	0.0	−0.161	−0.228	−0.187	−0.166	−0.148
$PH_3{}^b$	0.0	−0.031	−0.280	[b]		
Beg^a	0.0	0.238	0.243	0.220	0.154	−0.417
Beg^b	0.0	0.071	0.018	−0.025	0.055	0.017

(B) trans-metalation of Pd(OH)(Ph)$(PH_3)_2$ via dissociative substitution of PH_3 for $B_2(eg)_2$

	4	**9**	**10**	**11**	**12**	**TS$_{12-13}$**	**13**
Pd	0.0	−0.159	−0.086	−0.145	−0.182	−0.144	0.019
OH	0.0	−0.023	−0.095	−0.045	−0.195	−0.216	−0.260
Beg^a	0.0	0.0	0.0	−0.004	0.230	0.159	−0.432
Beg^b	0.0	0.0	0.0	−0.060	0.009	0.102	0.196

(C) trans-metalation of PdCl(Ph)$(PH_3)_2$ via associative substitution of PH_3 for $B_2(eg)_2$

	4Cl	**5Cl**	**TS$_{5Cl-6Cl}$**	**6Cl**	**TS$_{6Cl-7Cl}$**	**7Cl**
Pd	0.0	−0.011	−0.226	−0.192	−0.118	−0.063
Cl	0.0	0.023	0.031	0.029	−0.054	−0.323
$PH_3{}^b$	0.0	0.005	0.293			
Beg^a	0.0	0.001	−0.006	−0.006	−0.055	−0.162
Beg^b	0.0	0.003	−0.041	−0.076	−0.048	−0.081

(D) trans-metalation of PdCl(Ph)$(PH_3)_2$ via dissociative substitution of PH_3 for $B_2(eg)_2$

	4Cl	**9Cl**	**10Cl**	**11Cl**	**TS$_{12Cl-13Cl}$**	**13Cl**
Pd	0.0	−0.190	−0.066	−0.129	−0.110	−0.016
OH	0.0	0.010	−0.081	−0.027	−0.422	−0.483
Beg^a	0.0	0.0	0.0	−0.009	0.106	−0.234
Beg^b	0.0	0.0	0.0	−0.053	0.133	0.239

[a] Positive values represent that the population increases (vice versa). [b] Because $PH_3{}^b$ completely dissociates from the Pd center in **6**, **TS$_{6-7}$**, and **7**, we omitted its population change in these species.

The B−B bond scission takes place in the process from **6** to **7**. In this process, the electron population of Beg^a substantially decreases and that of Beg^b somewhat increases, where Beg^a and Beg^b form bonding interactions with OH and the Pd center, respectively (see Figure 1). Also, the electron populations of Pd and $PH_3{}^b$ substantially increase. These population changes provide well understanding of the electronic process of the B−B bond scission, as follows: Because Beg^a becomes bound with the electronegative OH group in the trans-metalation, Beg^a becomes positively charged, which induces polarization of $B_2(eg)_2$ to increase the electron population of Beg^b. Also, Beg^b should become negatively charged because it coordinates with the Pd center after the B−B bond scission. Thus, it is concluded that the B−B bond scission occurs in a heterolytic manner. However, Beg^b does not keep the whole electron population that is transferred from Beg^a but donates some of the electron population to the Pd center, to form the Pd−Beg^b coordinate bond. The Pd−Beg^b coordinate bond then suppresses the electron donation from $PH_3{}^b$ and Ph ligands to the Pd center, which leads to increases in electron population of these ligands. The above-mentioned polarization of the B−B bond is similar to that of the C−H bond of benzene in the heterolytic C−H σ-bond activation by Pd(η^2-$O_2CH)_2$.[56]

(56) Biswas, B.; Sugimoto, M.; Sakaki, S. *Organometallics* **2000**, *19*, 3895.

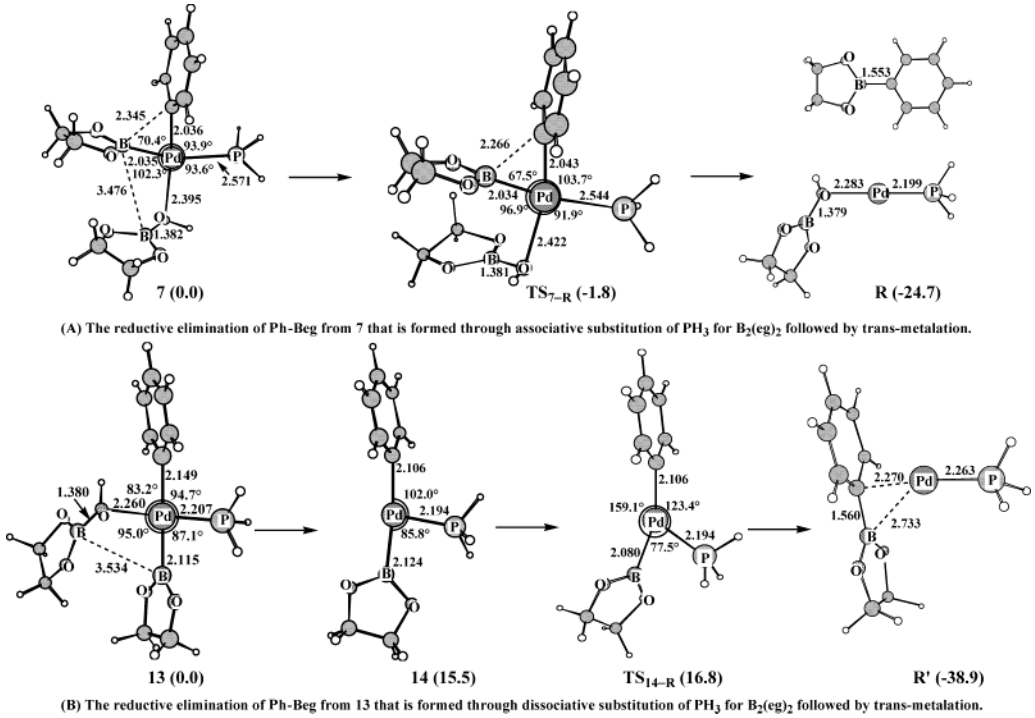

Figure 4. Geometry and energy changes by reductive eliminaiton of phenylborane. Bond lengths are in Å and bond angles are in degree. Relative energies to the sums of reactants (the DFT/BS-II method; kcal/mol unit) are in parentheses.

The similar population changes are observed in the trans-metalation process that takes place after the dissociative substitution of PH_3 for $B_2(eg)_2$ (see Table 1B). The discussion is omitted here not to repeat the similar discussion.

Reductive Elimination of Phenylborane, Ph−Beg. The final step is the reductive elimination of phenylborane, Ph−Beg. Pd(Beg)(Ph)(PH_3)(HO−Beg) **7** is a product of the associative substitution followed by the trans-metalation. From **7**, the reductive elimination proceeds through the transition state $\mathbf{TS_{7-R}}$, to afford Ph−Beg and Pd(PH_3)(HO−Beg), as shown in Figure 4(A). In $\mathbf{TS_{7-R}}$, the B−C distance between Beg and Ph ligands becomes somewhat shorter by 0.079 Å, whereas the Beg and Ph ligands little change their directions toward each others. The Pd−O distance slightly lengthens by 0.027 Å. These geometrical features indicate that this transition state is reactant-like. Consistent with the reactant-like transition state, the E_a value is nearly zero (−1.8 kcal/mol); note that the negative E_a value results from artificial error due to insufficient threshold of geometry optimization but it clearly shows that this reaction proceeds with a very small E_a value.

Complex **13** is a product of the dissociative substitution followed by the trans-metalation. In **13**, HO−Beg[a] must dissociate from the Pd center prior to the reductive elimination of Ph−Beg[a], because HO−Beg[a] takes a position between Ph and Beg ligands to inhibit the mutual approach of these two ligands, as shown in Figure 4(B). This dissociation occurs with considerably large destabilization energy of 15.5 kcal/mol. After that, the reductive elimination occurs with nearly no barrier (1.3 kcal/mol).

From these results, it should be reasonably concluded that the reductive elimination is not a rate-determining process. This is because the palladium(0) complex has d orbitals at low energy and is favorable for the reductive elimination, as well-known.[14,17b,c]

Trans-metalation of the Palladium(II) Chloro Phenyl Complex, PdCl(Ph)(PH_3)$_2$ 4Cl, with Diboron, $B_2(eg)_2$. It was experimentally reported that the basic condition accelerated the palladium-catalyzed borylation of aryl halide with diboron.[10] In similar cross-coupling reaction, it was also reported that PdCl(vinyl)(PR_3)$_2$ did not undergo the cross-coupling reaction with the organic boron ester but the methoxo analogue easily underwent it.[44a] To clarify the ligand effects in the trans-metalation, we investigate here the trans-metalation of PdCl(Ph)(PH_3)$_2$ **4Cl** with $B_2(eg)_2$. From **4Cl**, the associative substitution followed by the trans-metalation proceeds through geometry changes shown in Figure 5. Although the transition state $\mathbf{TS_{5Cl-6Cl}}$ of the PH_3 dissociation is essentially the same as $\mathbf{TS_{5-6}}$ of the OH analogue, the precursor complex **5Cl**, the transition state $\mathbf{TS_{6Cl-7Cl}}$, and the product **7Cl** considerably differ from the corresponding species of the OH system, as follows: In **5Cl**, $B_2(eg)_2$ does not interact with the Cl ligand, while it forms a considerably strong bonding interaction with the OH ligand in **5**. Consistent with the absence of the bonding interaction between the Cl ligand and $B_2(eg)_2$, **5Cl** is moderately more stable than **4Cl**, while **5** is much more stable than **4** in the OH system, which will be discussed below. The transition state $\mathbf{TS_{6Cl-7Cl}}$ of the Cl system is considerably different from $\mathbf{TS_{6-7}}$ of the OH system, as follows: (1) In $\mathbf{TS_{6Cl-7Cl}}$, any Beg group does not interact with the Cl ligand, while the Beg[a] group keeps a strongly bonding interaction with the OH ligand in $\mathbf{TS_{6-7}}$. (2) In $\mathbf{TS_{6Cl-7Cl}}$, two boryl groups seem to interact with the Pd center. This structure suggests that the Pd center takes +4 oxidation state; in other words, the B−B bond scission proceeds in a homolytic manner. In the product **7Cl,** the Beg[a] group interacts with both the Cl ligand and the O^{boryl} atom of Beg[b], while the Beg[a] group strongly interacts with only the OH ligand in **7**. This is reasonably interpreted in terms that the Beg[a] group still needs a charge-transfer interaction with the lone pair

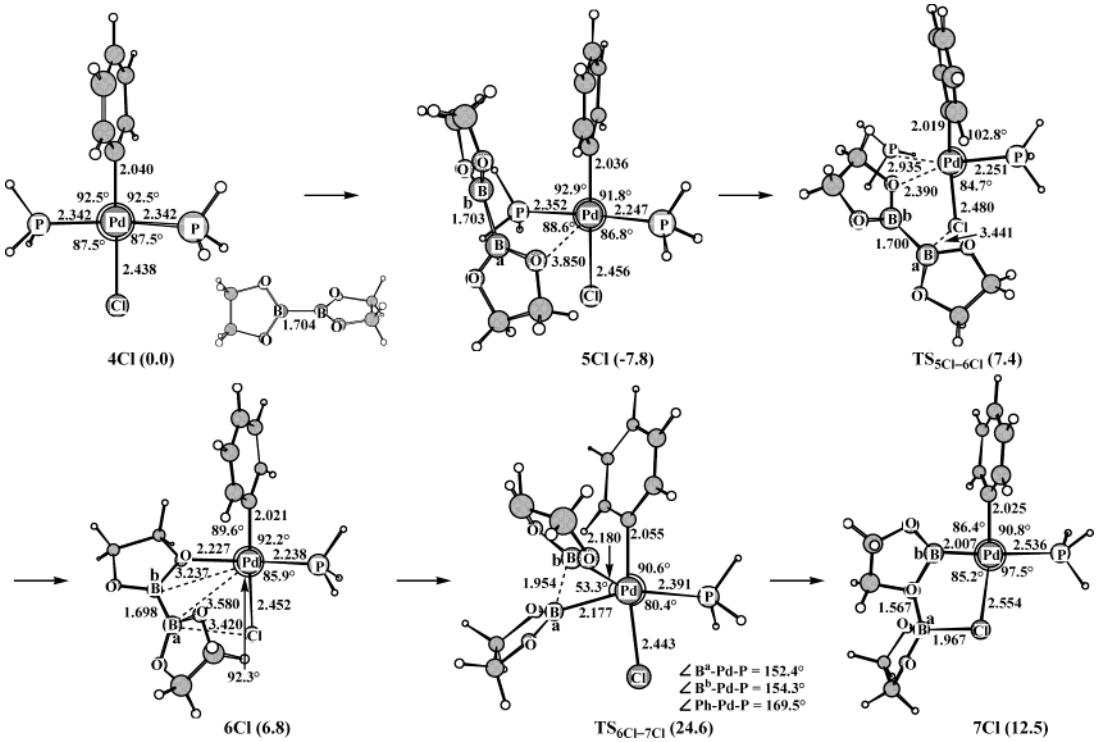

Figure 5. Geometry and energy changes by associative substitution of PH_3 for diboron, $B_2(eg)_2$, followed by trans-metalation in $PdCl(Ph)(PH_3)_2$. Bond lengths are in Å and bond angles are in degree. Relative energies to the sums of reactants (the DFT/BS−II method; kcal/mol unit) are in parentheses.

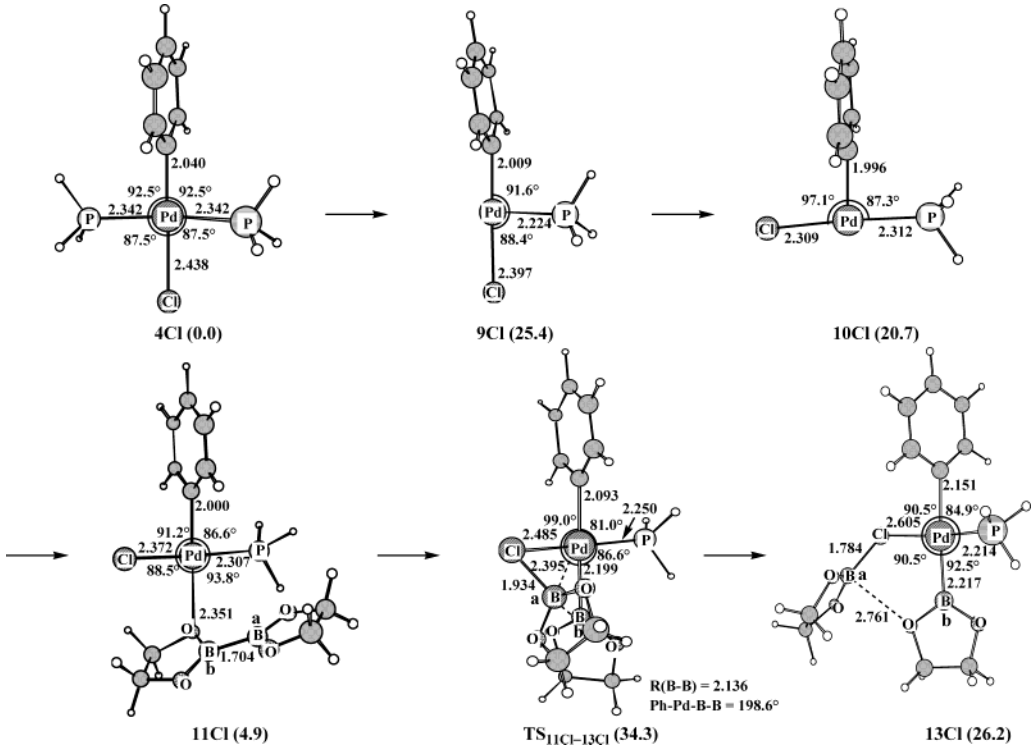

Figure 6. Geometry and energy changes by dissociative substitution of PH_3 for diboron, $B_2(eg)_2$, followed by trans-metalation in $PdCl(Ph)(PH_3)_2$. Bond lengths are in Å and bond angles are in degree. Relative energies to the sums of reactants (the DFT/BS-II method; kcal/mol unit) are in parentheses.

orbital of the O atom of the Beg^b group since the bonding interaction between the Beg^a group and the Cl ligand is not sufficiently strong, as discussed above. All of these features arise from the fact that the Cl ligand is less donating than the OH ligand.

The dissociative substitution followed by the trans-metalation of $PdCl(Ph)(PH_3)_2$ **8** takes place, as shown in Figure 6. Complex **8** undergoes dissociation of PH_3 from the Pd center to afford $PdCl(Ph)(PH_3)$ **9Cl** in which Cl is at a position trans to Ph. Complex **10Cl**, in which Cl is at a position cis to Ph, is more stable than **9Cl** by 4.7 kcal/mol. This isomerization from **9Cl** to **10Cl** easily occurs with a very small activation barrier of about 0.4 kcal/mol.[54a] $B_2(eg)_2$ approaches the Pd center of **10Cl**, to afford an adduct $PdCl(Ph)(PH_3)[B_2(eg)_2]$ **11Cl**. In **11Cl**, B_2-

$(eg)_2$ coordinates with the Pd center through the lone pair orbital of the O^{boryl} atom.[50] Although the intermediate **12** was optimized in the OH system, the similar intermediate could not be optimized in the Cl system. This is because the Cl ligand does not have enough ability to form a bonding interaction with the Beg group, of which reason will be discussed below. Thus, the B−B bond scission takes place upon going from **11Cl** to Pd(Beg^b)(Ph)(PH_3)(Cl−Beg^a) **13Cl** through the transition state **TS$_{11Cl-13Cl}$**. In **TS$_{11Cl-13Cl}$**, the Pd−Beg^b distance is 2.199 Å, which suggests that the Pd−Beg^b bond has been almost formed. The other Beg^a group, that is approaching the Cl ligand, changes its direction from the Beg^b group toward the Pd center. The Cl−Beg^a distance is still long (1.934 Å), which represents that the covalent bond between the Beg^a group and the Cl ligand has not been formed in this transition state. The rather short Pd−Beg^a distance (2.395 Å) indicates that some bonding interaction is formed between the Pd center and the Beg^a group. On the other hand, the long B−B distance (2.136 Å) indicates that the B−B bond is almost broken in this transition state. These geometrical features suggest that four anion ligands coordinate with the Pd center in **TS$_{11Cl-13Cl}$**; in other words, the Pd center takes +4 oxidation state in this transition state like that in **TS$_{6Cl-7Cl}$** of the trans-metalation via the associative substitution. Consistent with this suggestion, **TS$_{11Cl-13Cl}$** takes a distorted square pyramidal structure in which the Cl and PH_3 ligands are at axial positions and the Ph and two Beg groups are on the equatorial plane; actually, the dihedral angle (199°) between the Ph−Pd−B plane and the Pd−B−B plane is close to 180°. In **13Cl**, Cl−Beg^a weakly coordinates with the Pd center, where the Pd−Cl distance (2.605Å) is much longer than that of **4Cl**. This structure is somewhat different from **7Cl**, as follows: The B−O^{boryl} distance (2.761Å) between Cl−Beg^a and the Beg^b group is very long in **13Cl**, whereas **7Cl** possesses a strongly bonding interaction between Cl−Beg^a and Beg^b.

Significant difference in the population change is observed between the Cl and OH systems. As shown in Table 1, parts C and D, the electron populations of Beg^a and Beg^b are similar to each other in **TS$_{6Cl-7Cl}$** and **TS$_{12Cl-13Cl}$** of the Cl system, whereas the electron population of Beg^a decreases but that of Beg^b increases in **TS$_{6-7}$** and **TS$_{12-13}$** of the OH system. These similar electron populations of Beg^a and Beg^b in the Cl system are consistent with the above-discussed feature that the B−B bond scission occurs in a homolytic manner in the Cl system. The discussion of the other population changes is omitted here for brevity (see Supporting Information Figures S-6−S-8).

Energy changes by the associative substitution followed by the trans-metalation are shown in Figure 7. The activation barrier of the PH_3 substitution is calculated to be 15.2 kcal/mol. This activation barrier is similar to that of the PH_3 substitution in Pd(OH)(Ph)$(PH_3)_2$. In the next step, the B−B bond scission occurs through **TS$_{6Cl-7Cl}$** with a considerably large activation barrier of 17.8 kcal/mol, which is 2 times as large as that of the OH system. Because **6Cl** is only slightly more stable in energy than **TS$_{5Cl-6Cl}$**, the real activation barrier to reach **7Cl** from **5Cl** corresponds to the energy difference between **TS$_{6Cl-7Cl}$** and **5**. This value (32.4 kcal/mol) is substantially large. Thus, the associative substitution followed by the trans-metalation is much more difficult in PdCl(Ph)$(PH_3)_2$ than that of the OH analogue. The reasons are easily understood by comparing the geometry of **TS$_{6Cl-7Cl}$** with that of **TS$_{6-7}$**, as follows: The HO−Beg^a bonding interaction is formed in **6** and **TS$_{6-7}$** of the OH system. This means that the B−B bond of **6** is weakened by the HO−Beg^a bonding interaction. Moreover, the HO−Beg^a bonding interaction becomes stronger upon going from **6** to **7**, to compensate the destabilization induced by the B−B bond breaking. Actually, the HO−Beg^a distance becomes shorter upon going to **7** from **6**, as discussed above (see also Figure 1). Also, this bonding interaction induces the polarization of $B_2(eg)_2$, which facilitates the heterolytic B−B bond scission. In **6Cl** and **TS$_{6Cl-7Cl}$**, on the other hand, the Beg^a group cannot form a bonding interaction with the Cl ligand. Thus, the energy destabilization by the B−B bond breaking cannot be compensated by the strengthening of the Cl−Beg bonding interaction. Also, the heterolytic B−B bond scission becomes difficult because of the absence of the interaction between $B_2(eg)_2$ and the Cl ligand. As a result, the B−B bond scission must proceed in a homolytic manner. In the transition state of this homolytic B−B bond scission, the Pd center must take +4 oxidation state. This is very difficult because the Pd atom has d-orbitals at low energy.[14,17b,c] Thus, the trans-metalation in the Cl system requires much larger activation barrier than that of the OH system. This conclusion does not change, even if we discuss the results with the free energy change, as follows: The activation free energy change ($\Delta G_v^{0\ddagger}$) upon going to **TS$_{6Cl-7Cl}$** from **5Cl** is 34.0 kcal/mol. This is much larger than that (24.4 kcal/mol) of the OH system. If we adopt the $\Delta G°$ value in gas-phase reaction, the activation free energy change ($\Delta G^{0\ddagger}$) of the trans-metalation corresponds to the free energy difference between **TS$_{6Cl-7Cl}$** and **6Cl**. This value is 20.3 kcal/mol in the Cl system, which is much larger than the $\Delta G^{0\ddagger}$ value (11.3 kcal/mol) in the OH system. In both free energy estimations, the Cl system requires much larger $\Delta G^{0\ddagger}$ value than does the OH system.

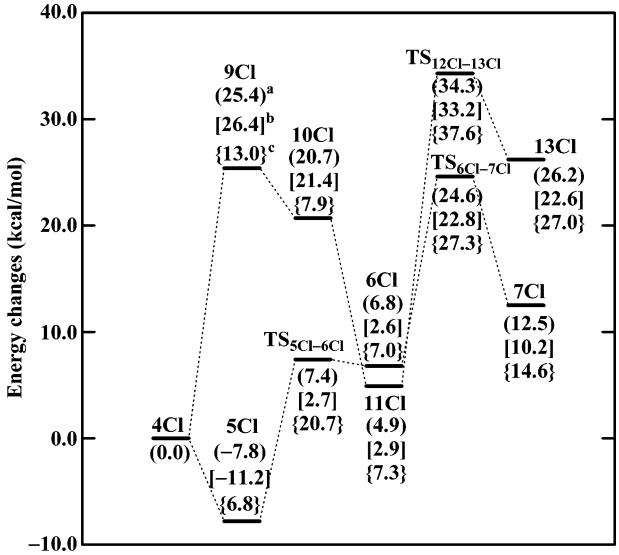

Figure 7. Energy changes in associative substitution of PH_3 for $B_2(eg)_2$ followed by trans-metalation and dissociative substitution followed by trans-metalation of PdCl(Ph)$(PH_3)_2$. The DFT/BS-II method; kcal/mol unit. (a) Potential energy changes. (b) Gibbs free energy changes (ΔG_v^0) at 298 K, where only vibration movements are taken into consideration in the estimation of free energy. (c) Gibbs free energy changes ($\Delta G°$) at 298 K in gas-phase reaction, where translation, rotation, and vibration movements are taken into consideration in the estimation of free energy.

Energy changes by the dissociative substitution followed by the trans-metalation of PdCl(Ph)$(PH_3)_2$ are shown in Figure 7, too. The PH_3 dissociation gives rise to considerably large

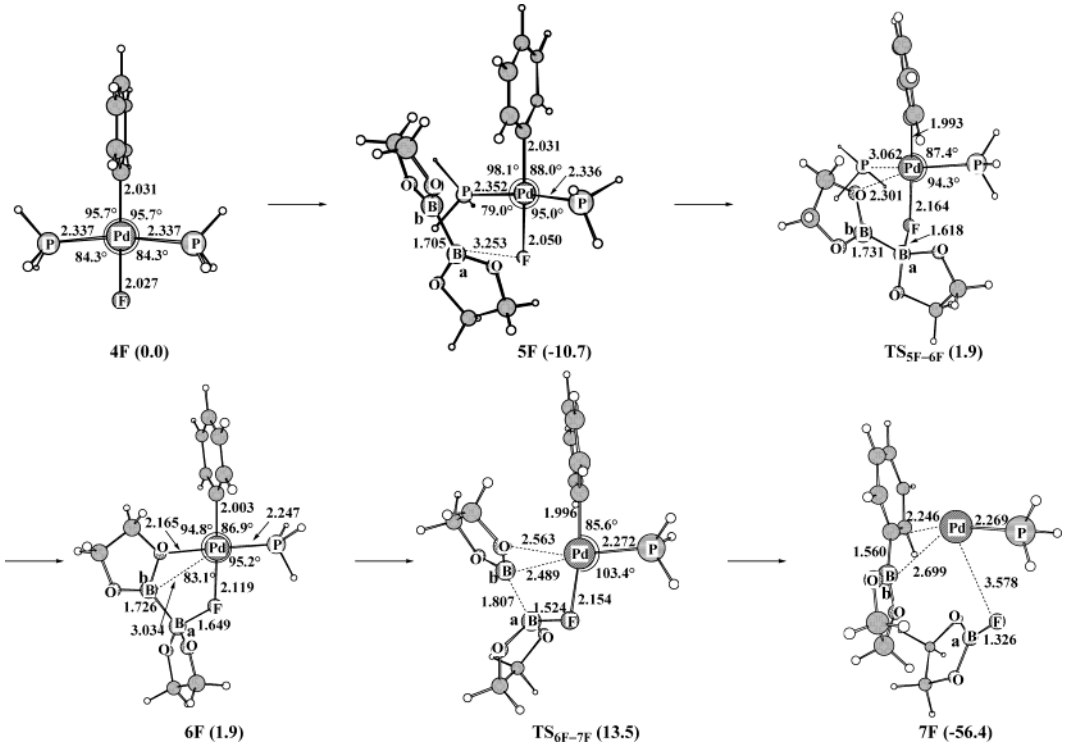

Figure 8. Geometry and energy changes by associative substitution of PH_3 for diboron, $B_2(eg)_2$, followed by trans-metalation in $PdF(Ph)(PH_3)_2$. Bond lengths are in Å and bond angles are in degree. Relative energies to the sums of reactants (the DFT/BS-II method; kcal/mol unit) are in parentheses.

destabilization energy of 25.4 kcal/mol, which is similar to the destabilization energy of the OH system. The isomerization from **9Cl** to **10Cl** takes place with nearly no barrier (0.02 kcal/mol),[54a] like that of the OH system. $B_2(eg)_2$ interacts with **10Cl**, to afford **11Cl**. One significant difference between **11** and **11Cl** is that the energy stabilization by coordination of $B_2(eg)_2$ is smaller in **11Cl** than that in **11**. The next step is the B−B bond scission which needs a considerably large E_a value of 29.4 kcal/mol. The $\Delta G^{0\ddagger}$ value of this step is also very large; $\Delta G^{0\ddagger}$ in gas phase is 30.3 kcal/mol and $\Delta G_v^{0\ddagger}$ is 30.3 kcal/mol. These values are much larger than those of the OH complex (7.9 and 8.0 kcal/mol, respectively). The reason is again attributed to the weak Cl−Beg bonding interaction, as discussed above.

From these results, it should be clearly concluded that the trans-metalation of $PdCl(Ph)(PH_3)_2$ occurs with much difficulty in both reaction course via the associative substitution and that via the dissociative one. This conclusion agrees well with the experimental result that the basic condition accelerates the palladium-catalyzed cross-coupling reaction of aryl halide with diboron[10] but $PdCl(vinyl)(PPh_3)_2$ is inert to the cross-coupling reaction with organic boron compound.[44a]

Trans-metalation of the Palladium(II) Fluoro Phenyl Complex, $PdF(Ph)(PH_3)_2$ 4F, with Diboron, $B_2(eg)_2$. Also, we investigate the trans-metalation of $PdF(Ph)(PH_3)_2$ **4F** with $B_2(eg)_2$, to elucidate the ligand effects in the trans-metalation. In the associative substitution of PH_3 for $B_2(eg)_2$, $B_2(eg)_2$ approaches **4F** to afford an adduct, $PdF(Ph)(PH_3)_2[B_2(eg)_2]$ **5F**, as shown in Figure 8. This adduct **5F** is essentially the same as **5Cl**, since the Beg^a group is considerably distant from the F ligand. However, the transition state, $\mathbf{TS_{5F-6F}}$, through which PH_3 is substituted for $B_2(eg)_2$, is much different from $\mathbf{TS_{5Cl-6Cl}}$ of the Cl system but essentially the same as $\mathbf{TS_{5-6}}$ of the OH system. For instance, the F−Beg^a distance (1.639 Å) is rather short in $\mathbf{TS_{5F-6F}}$ like that of the OH system. The transition state $\mathbf{TS_{5F-6F}}$ takes a trigonal bipyramidal structure, which is a typical transition state of the associative substitution in the d^8 metal system. In the intermediate $PdF(Ph)(PH_3)[B_2(eg)_2]$ **6F**, the F−Beg^a distance is short (1.651 Å) and the Beg^b group coordinates to the Pd center with the lone pair orbital on the O^{boryl} atom of Beg^b like that of **6**.[50] The B−B bond scission of **6F** takes place through the transition state $\mathbf{TS_{6F-7F}}$, to afford $Pd(Ph-Beg^b)(PH_3)(F-Beg^a)$ **7F**. Complex **7F** is a final product after the reductive elimination of Ph−Beg. This means that the reductive elimination very easily occurs in the fluoro system, probably because the Ph and Beg groups take positions cis to each other and F−Beg^a does not coordinate well with the Pd center not to stabilize *cis*-$Pd(Ph)(Beg^b)(PH_3)(F-Beg^a)$.

Geometry changes in the dissociative substitution followed by the trans-metalation are shown in Figure 9. Complex **4F** undergoes the PH_3 dissociation from the Pd center, to afford $Pd(F)(Ph)(PH_3)$ **9F** of which geometry is similar to those of **9** and **9Cl**. Complex **10F**, in which the F ligand is at a position cis to the Ph ligand, is somewhat more stable than **9F**. $B_2(eg)_2$ coordinates with the Pd center of **11F** through the lone pair orbital on the O^{boryl} atom of Beg^b. In **12F**, $B_2(eg)_2$ interacts with both the Pd center and the F ligand, like that of **12**, whereas **12F** is less stable than **11F**.[54b] In **12F**, the B−B bond scission occurs through the transition state $\mathbf{TS_{12F-13F}}$ to afford an intermediate Pd(II) complex, $Pd(Ph)(Beg^b)(PH_3)(F-Beg^a)$ **13F**. The geometry of $\mathbf{TS_{12F-13F}}$ well resembles that of $\mathbf{TS_{6F-7F}}$. In this reaction course, the intermediate **13F** is formed unlike the reaction course via the associative substitution. This is because F−Beg^a takes a position between Ph and Beg^b ligands to suppress the reductive elimination of Ph−Beg^b. In other words, the reductive elimination cannot proceed without the dissociation of F−Beg^a from the Pd center in **13F**. The dissociation of

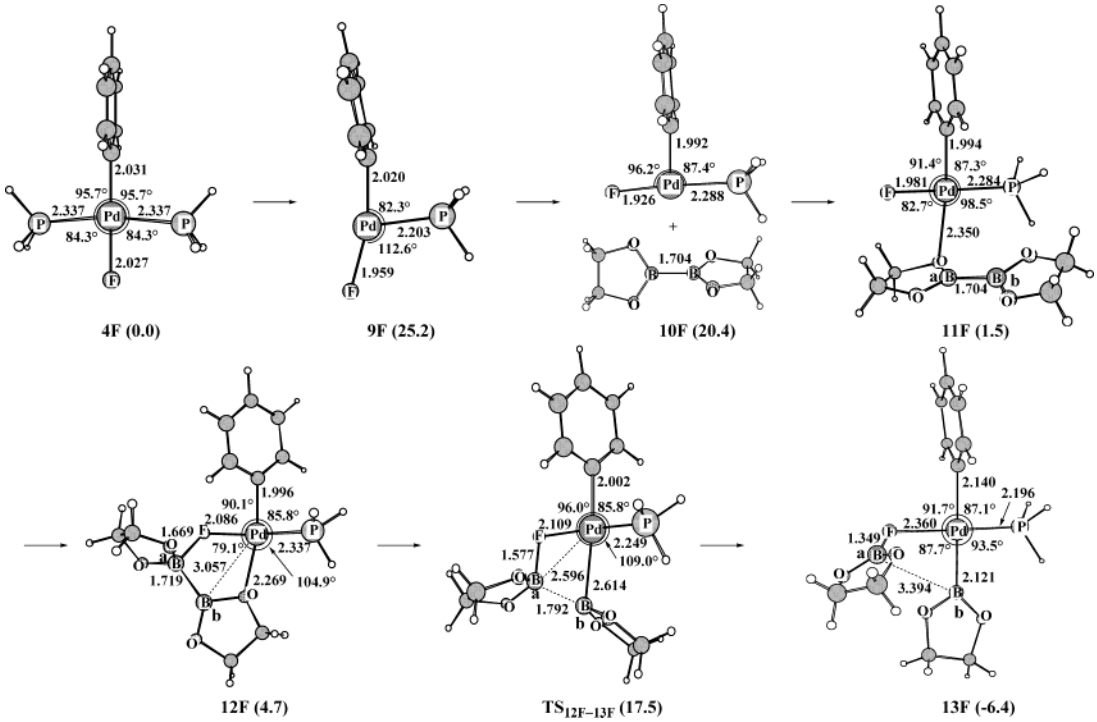

Figure 9. Geometry and energy changes by dissociative substitution of PH_3 for diboron, $B_2(eg)_2$, followed by trans-metalation in $PdF(Ph)(PH_3)_2$. Bond lengths are in Å and bond angles are in degree. Relative energies to the sums of reactants (the DFT/BS-II method; kcal/mol unit) are in parentheses.

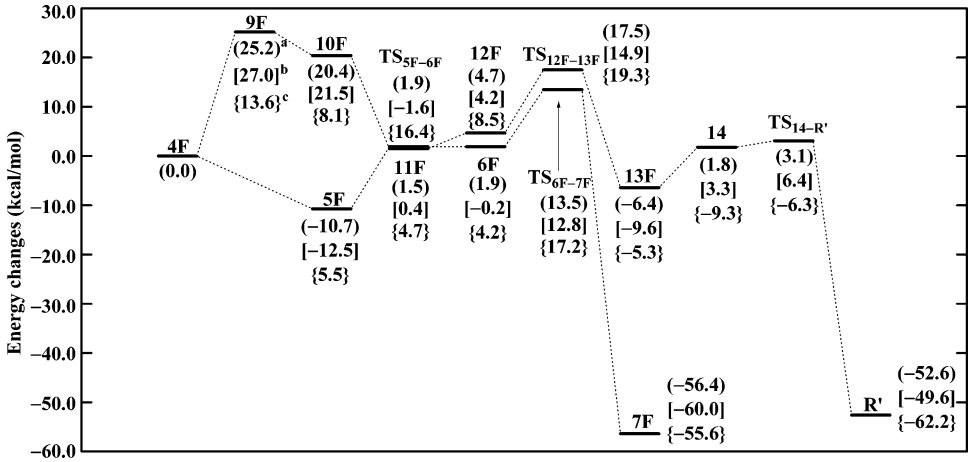

Figure 10. Energy changes in associative substitution of PH_3 for $B_2(eg)_2$ followed by trans-metalation and dissociative substitution followed by trans-metalation of $PdF(Ph)(PH_3)_2$. The DFT/BS-II method; kcal/mol unit. (a) Potential energy changes. (b) Gibbs free energy changes (ΔG_v^0) at 298 K, where only vibration movements are taken into consideration in the estimation of free energy. (c) Gibbs free energy changes ($\Delta G°$) at 298 K in gas-phase reaction, where translation, rotation, and vibration movements are taken into consideration in the estimation of free energy.

F−Beg[a] occurs with moderate destabilization energy of 8.2 kcal/mol. After the dissociation, the reductive elimination easily takes place like that of the OH system, as discussed above.

Energy changes by these two reaction courses are shown in Figure 10. In the associative substitution followed by the trans-metalation, $B_2(eg)_2$ interacts with **4F** to yield the stabilization energy of 10.7 kcal/mol. The E_a value for the PH_3 substitution is 12.6 kcal/mol. Although the trans-metalation (**6F** → **7F**) occurs with the moderate E_a value of 11.6 kcal/mol, the total E_a value of the process from 5**F** to **7F** corresponds to the energy difference between **5F** and $\mathbf{TS_{6F-7F}}$, because **6F** is only slightly more stable than $\mathbf{TS_{5F-6F}}$ like that of the OH system. This E_a value is 24.2 kcal/mol, which is similar to that (24.0 kcal/mol) of the OH system but much smaller than that (32.4 kcal/mol) of the Cl system.

In the dissociative substitution followed by the trans-metalation, the first step is the dissociation of PH_3 from the Pd center, which gives rise to a very large destabilization energy of 25.2 kcal/mol like that of the other systems. The isomerization from **9F** to **10F** easily occurs with nearly no barrier (1.7 kcal/mol with the DFT/BS−I method and −0.4 kcal/mol with the DFT/BS−II method).[54a] The coordination of $B_2(eg)_2$ with **10F** leads to **11F** with a considerably large stabilization energy of 18.9 kcal/mol. The trans-metalation requires the E_a value of 12.8 kcal/mol. This E_a value is moderately larger than that (9.1 kcal/mol) of the OH system but much smaller than that (29.4 kcal/mol) of the Cl system, too. Thus, it should be clearly concluded that the trans-metalation of the F system can take place with a similar E_a value to that of the OH system. The discussion based on the ΔG_v^0 value provides the same conclusion, which is

omitted here. Because the trans-metalation of the F system induces similar population changes to those of the OH system, the discussion of population changes is omitted here, too (see Supporting Information Figure S-8).

Summary of Energy Changes. The first step is the oxidative addition of aryl halide to the palladium(0) complex. The products are *cis*- and/or *trans*-Pd(I)(Ph)$(PH_3)_2$. As discussed above, it is likely to consider experimentally that both the isomerization from the cis form to the trans form and the substitution of halide for OH^- easily take place.[2a,53] Actually, *trans*-Pd(OH)(Ph)$(PH_3)_2$ is much more stable than *trans*-Pd(I)-(Ph)$(PH_3)_2$ by 35.1 kcal/mol in diethyl ether. The next step is either the associative substitution of PH_3 for $B_2(eg)_2$ or the dissociative substitution of PH_3 for $B_2(eg)_2$. $B_2(eg)_2$ can form a stable adduct with Pd(OH)(Ph)$(PH_3)_2$ and PdF(Ph)$(PH_3)_2$, because $B_2(eg)_2$ exists in excess under the catalytic reaction conditions. On the other hand, the dissociation of PH_3 from the Pd center gives rise to significantly large destabilization energy. Thus, the associative substitution takes place more easily than does the dissociative substitution. The discussion based on the ΔG_v^0 value leads to the same conclusion, as discussed above, whereas the $\Delta G°$ value leads to the different conclusion that the reaction via the dissociative substitution more easily occurs than that via the associative one in gas phase. After the dissociative substitution, the trans-metalation of Pd(OH)(Ph)-$(PH_3)[B_2(eg)_2]$ takes place to afford Pd(Beg)(Ph)(PH_3)(HO−Beg). The final step is the reductive elimination of Ph-Beg which easily proceeds with nearly no barrier in the reaction course via the associative substitution. In the reaction course via the dissociative substitution, the X-Beg moiety must dissociate from the Pd center with considerable destabilization energy of about 8 kcal/mol, and then the reductive elimination proceeds with nearly no barrier.

The free energy changes by the reaction via the associative substitution are summarized here, while the free energy changes by the reaction via the dissociative substitution are omitted because this reaction course is less favorable than that via the associative substitution in solution. The ΔG_v^0 value provides almost the same energy changes as those of potential energy changes. The $\Delta G_v^{0‡}$ value of the trans-metalation increases in the order OH (24.4) < F (25.3) ≪ Cl (34.0) and the ΔG_v^0 value also increases in the order F (−60.0) < OH (−54.5) ≪ Cl (10.2), where parentheses are $\Delta G_v^{0‡}$ and ΔG_v^0 values (in kcal/mol), respectively. These results agree with the experimental results that the basic condition accelerates this cross-coupling reaction[10] and that Pd(OMe)(vinyl)$(PPh_3)_2$ undergoes the cross-coupling reaction with organic boron compound but the Cl analogue does not.[44] These results lead to theoretical prediction that not only the basic condition but also addition of fluoride anion accelerates this catalytic reaction.

Here, we wish to mention the second catalytic cycle. Since the product of the reductive elimination is Pd(PH_3)(L) (L = HO−Beg or Ph−Beg), there are several possibilities in the second cycle. If phosphine coordinates with the Pd center, then the second cycle is the same as the first cycle. If the oxidative addition of iodobenzene to Pd(PH_3)(L) occurs, the second cycle becomes different from the first one. Also, coordination of either $B_2(eg)_2$ or Lewis base such as OAc^- and OH^- with the Pd(0) center changes the catalytic cycle. Actually, coordination of Lewis base with the Pd(0) center was experimentally reported.[57] Thus, the second cycle depends on the coordination abilities of phosphine, $B_2(eg)_2$, and OH^-, the reactivity of iodobenzene, and the reaction conditions. The investigation of the second cycle needs a long CPU time, and it will be investigated in a near future. However, Pd(OH)(Ph)$(PH_3)[B_2(eg)_2]$ is formed in all these cases and the trans-metalation process occurs in the similar way to that of the first cycle.

Table 2. Bond Energies of the X−Beg, Pd−X, and Pd−(X−Beg) Bonds

(A) X−Beg bond energy[a]

	HO	F	Cl	I
DFT	147.3	166.4	118.5	86.2
MP2	152.9	169.0	123.4	90.5
MP3	146.3	161.3	120.5	87.5
MP4(DQ)	145.9	161.5	119.0	86.3
MP4(SDQ)	151.7	162.3	119.2	91.7
CCSD	145.4	161.4	118.6	
CCSD(T)	147.0	162.9	120.3	

(B) Pd−X and Pd−(X−Beg) bond energies[b]

	Pd–X	Pd–(X–Beg)
HO	66.0	15.5
Cl	81.0	10.1
F	93.6	8.2

[a] In kcal/mol. BS-II was used, where the geometries were optimized with the DFT/BS-I method. [b] In kcal/mol. The DFT/BS-II//DFT/BS-I method was used.

Reasons of Differences between the Cl Ligand and Such Lignads as OH and F. It is of considerable importance to clarify the reason that the palladium chloro complex does not undergo the trans-metalation with diboron but the fluoro and hydroxo complexes easily undergo it. In the trans-metalation, the Pd−X and B−B bonds are broken, while the X−Beg and Pd−Beg bonds are formed. Also, X−Beg still coordinates with the Pd center in the product. Thus, we must consider the Pd−X, X−Beg, and Pd−(X−Beg) bond energies in the discussion. The X−Beg bond energy was evaluated with eq 1, where geometries of ·Beg and ·X were optimized with the DFT/BS−I method.

$$\text{X−Beg} \rightarrow \cdot\text{X} + \cdot\text{Beg} \quad (1)$$

As shown in Table 2, the F−Beg and HO−Beg bond energies are significantly large, while the Cl−Beg bond energy is small. The I−Beg bond energy is further smaller than the Cl−Beg bond energy. The Pd−X bond energy was defined as energy difference between Pd(X)(Ph)$(PH_3)_2$ and the sum of ·Pd(Ph)-$(PH_3)_2$ and ·X (see eq 2), where

$$\textit{trans}\text{-PdX(Ph)}(PH_3)_2 \rightarrow \textit{trans}\text{-}\cdot\text{Pd(Ph)}(PH_3)_2 + \cdot\text{X} \quad (2)$$

$$\textit{cis}\text{-Pd(Ph)(Beg)}(PH_3)\text{(X-Beg)} \rightarrow \textit{cis}\text{-Pd(Ph)(Beg)}(PH_3) + \text{X-Beg} \quad (3)$$

·Pd(Ph)$(PH_3)_2$ and ·X were calculated with the DFT/BS−II//DFT/BS−I method. This bond energy becomes stronger in the order Pd−I < Pd−OH < Pd−Cl < Pd−F. The Pd−(X-Beg) bond energy was defined as the energy difference between the left-hand side and the right-hand side of eq 3, where the DFT/BS−II//DFT/BS−I method was used. This bond becomes

(57) Amatore, C.; Jutand, A.; Thuilliez, A. *Organometallics* **2001**, *20*, 3241.

Table 3. Orbital Energies of HO, F, Cl, I, and Beg, and Ionization Potential of X^- [a]

	HO	F	Cl	I	Beg
orbital energy of neutral radical[b]	−11.13	−15.0	−11.13	−9.11	−6.08
orbital energy in $PdX(Ph)(PH_3)_2$[c]	−10.25	−11.4	−9.93		
NBO charge of X in $PdX(Ph)(PH_3)_2$[d]	−0.713	−0.786	−0.699		
ionization potential of X^- [e]	−0.16	1.39	2.18	2.46	
	(0.26)	(1.85)	(2.75)	(2.95)	

[a] Hartree−Fock orbital calculated with the BS−II set. [b] Energies (eV) of singly occupied orbital of F, Cl, and I atoms and OH radical. [c] The lone pair orbital energy in $PdX(Ph)(PH_3)_2$. [d] The DFT/BS-II method. [e] The ΔSCF calculation with the CCSD(T) method. In parentheses are the DFT-calculated values.

Scheme 4

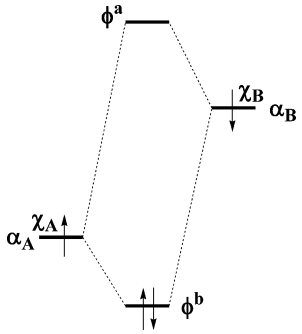

weaker in the order HO−Beg > Cl−Beg > F−Beg, as shown in Table 2. When X is OH, the weak Pd−OH bond is broken but the very strong HO−Beg bond is formed. Also, Pd−(HO−Beg) bond is strongest in these species. Although the Pd−F bond is somewhat stronger than the Pd−Cl bond by 12.6 kcal/mol and the Pd−(F−Beg) bond is slightly weaker than the Pd−(Cl−Beg) bond by 1.9 kcal/mol, the F−Beg bond is much stronger than the Cl−Beg bond. Thus, the product of the trans-metalation is the most stable when X is either OH or F.

The next issue is to explain these results of bond energy. Because the reactivity of trans-metalation mainly depends on the X−Beg bond energy, we wish to concentrate on the X−Beg bond here. On the basis of Hückel theory, the stabilization energy (ΔE_{cov}) of

$$\Delta E_{cov} = \epsilon_B - \epsilon_B + \beta^2/(\epsilon_B - \epsilon_A) \qquad (4)$$

the covalent bond formation is given by eq 4, when two orbitals, χ_A and χ_B, are well separated in energy.[27b,58] In eq 4, ϵ_A and ϵ_B are orbital energies of χ_A and χ_B, respectively (see Scheme 4), and β is a usual resonance integral. This simple eq indicates that the ΔE_{cov} value increases with an increase in energy difference between ϵ_A and ϵ_B. The valence orbital of the Beg group is at a higher energy than those of the F, Cl, and I atoms and that of the OH group, as shown in Table 3. This means that the X−Beg bond energy becomes larger as the valence orbital of X becomes lower in energy. The orbital energy becomes higher in the order F < OH ≈ Cl < I, which indicates that the σ-covalent bond becomes stronger in the order I < Cl ≈ OH < F. Besides the σ-covalent bond, the π bonding interaction is formed between the occupied p_π orbital of X and the unoccupied p_π orbital of Beg.[28] Actually, the occupied p_π orbital of OH and F can form stronger π-bonding interaction with the unoccupied p_π orbital of Beg than does the occupied p_π orbital of Cl, as shown in Figure 11.[59] The π bond is not formed well between I and Beg. Thus, the F and OH groups are more favorable than the Cl ligand. The I atom is the worst for the bonding interaction because its valence σ-orbital is at a high energy and the π bonding interaction with the Beg group is very weak.

In the transition state, the X-Beg σ-bond is not completely formed but the charge-transfer interaction between the X ligand and the Beg group is formed. Here, we investigate the bonding interaction between the X^- group and the empty p_π orbital of Beg. As shown in Table 3, the p_π orbital energy of X in $PdX(Ph)(PH_3)_2$ decreases in the order X = Cl > OH > F. Thus, these orbital energies suggest that the charge-transfer interaction becomes stronger in the order F < OH < Cl, which is not consistent with the strength of the bonding interaction between the X ligand and $B_2(eg)_2$. However, the ionization potential of X^- calculated with the ΔSCF method decreases in the order I^- > Cl^- > F^- > OH^-, which differs from the increasing order of orbital energy. This result suggests that the charge-transfer induces considerably large relaxation energy and that the OH ligand can form strong charge-transfer interaction with the Beg group, while its π orbital is at a lower energy than that of the Cl ligand. The next is the F ligand, and the Cl and I ligands are unfavorable for the charge-transfer interaction.

Also, the electrostatic interaction between the X ligand and the B atom of Beg contributes to the interaction between the X ligand and the Beg group. The negative charge of the X ligand increases in the order Cl < F < OH (see Table 3). Because the B atom of Beg is positively charged, the electrostatic interaction becomes stronger in the order Cl < F < OH. From all these factors, the interaction between the X ligand and the Beg group increases in the order Cl < F < OH.[60]

Conclusions

Trans-metalation process involved in the palladium-catalyzed borylation of iodobenzene with diboron was theoretically investigated with the DFT method. We investigated two reaction courses of trans-metalation; one is the associative substitution of the PH_3 ligand for $B_2(eg)_2$ followed by the trans-metalation and the other is the dissociative substitution followed by the trans-metalation. Because $B_2(eg)_2$ can form a considerably stable adduct with $PdX(Ph)(PH_3)_2$ when X is either OH or F, the associative substitution followed by the trans-metalation more easily occurs than does the dissociative substitution followed

(58) Biswas, B.; Sugimoto, M.; Sakaki, S. *Organometallics* **1999**, *18*, 4015.

(59) The B−O distance of the Beg moiety in X−Beg slightly depends on the p_π−p_π bonding interaction between the X and Beg groups; the B−O distance is 1.378Å in HO−Beg, 1.368Å in F−Beg, 1.364Å in Cl−Beg, and 1.360Å in I−Beg. These results clearly indicate that the π-bonding interaction between I and Beg groups is very weak.

(60) AcO−Beg bond energy is calculated to be 130.0 kcal/mol with the DFT/BS−II/DFT/BS−I method. This value is smaller than the HO−Beg and F−Beg bond energies but much larger than the Cl−Beg bond energy. Although the Pd−OAc and Pd−(AcO−Beg) bond energies should be considered in the discussion, the large AcO−Beg bond energy suggests that the palladium acetate complex is one of candidates of good catalysts. Actually, the AcO salt was experimentally used in the first report of Ishiyama et al.[10]

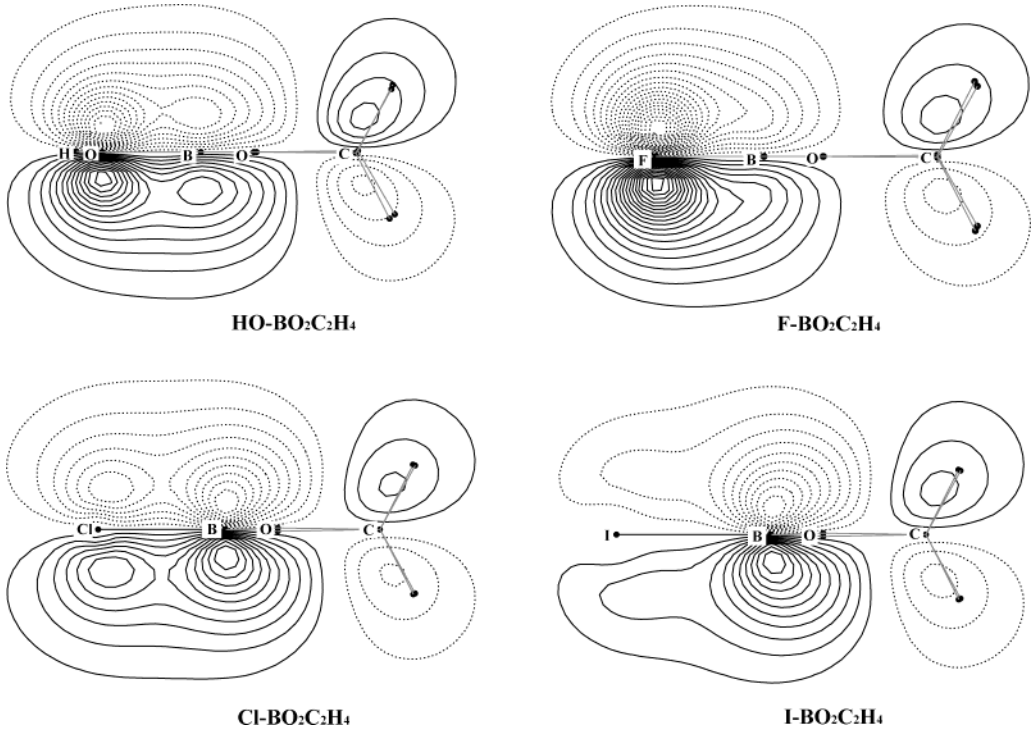

Figure 11. Contour maps of HOMO of X−Beg (X = OH, F, Cl, or I) Hartree−Fock calculation with BS-II. Contour values are 0.0, ±0.0125, ±0.025, ...

by the trans-metalation. This trans-metalation easily takes place through a four-center transition state with a moderate activation barrier, when either the OH ligand or the F ligand coordinates with the Pd center. In the transition state, the B−B bond breaking, the Pd−X (X = OH or F) bond weakening, and the Pd−Beg bond formation are in progress, and the X−Beg bonding interaction is becoming stronger. From these features, it should be concluded that the strengthening of the X−Beg bonding interaction compensates the weakening of the Pd−X and B−B bonds, to accelerate the trans-metalation. Also, this X−Beg interaction induces the polarization of $B_2(eg)_2$ to facilitate the heterolytic B−B bond scission. These results present the clear understanding of the experimental result that the basic condition accelerates the palladium-catalyzed borylation of aryl halide with diboron and lead to the prediction that the fluoro ligand induces the similar acceleration. The electron re-distribution in the trans-metalation also shows that the B−B bond scission occurs in a heterolytic manner. It is the other important feature of this trans-metalation. When the chloro ligand coordinates with the Pd center, on the other hand, the trans-metalation takes place with difficulty. This is because the chloro ligand cannot form the strongly bonding interaction with the Beg group. Actually, the Cl−Beg bond energy is much smaller than the HO−Beg and F−Beg bond energies. Because of the absence of the Cl−Beg interaction, the B−B bond scission occurs in a homolytic manner in the Cl system, which is very difficult in the Pd(II) complex. The final step is the reductive elimination of phenylborane. Since the reductive elimination occurs very easily, acceleration of this trans-metalation leads to more efficient palladium-catalyzed borylation of aryl halides with diboron.

In conclusion, the fundamental features of the trans-metalation process are clearly shown here. Our intention here is to present the first theoretical report of the trans-metalation of transition-metal complexes and the theoretical prediction that not only Lewis base but also the fluoro ligand accelerates the trans-metalation process. The successful result of this palladium-catalyzed borylation of aryl halides is attributed to the characteristic feature of the boryl group; it is the presence of the empty p_π orbital on the B atom with which the Beg group forms a bonding interaction with the X ligand to accelerate the heterolytic B−B bond scission. The similar features are expected to be observed in Suzuki−Miyaura coupling reaction, of which theoretical study is under progress now in our laboratory.

Acknowledgment. The authors wish to thank professors Miyaura and Ishiyama for the helpful discussion.This work was in part supported by Ministry of Education, Culture, Science, Technology, and Sports through Grant-in-Aids on priority areas of “Reaction Controle of Dynamic Complexes”, “Exploitation of Multi-Element Cyclic Molecules” (No.412 and 420), Grant-in-Aid for Creative Scientific Research, and NAREGI Project. All calculations were carried out SGI workstation in the Institute for Molecular Science (Okazaki, Japan) and Pentium IV-cluster systems of our laboratory.

Supporting Information Available: Table of ionization potential of HO^-, F^-, Cl^-, and I^- calculated with DFT, MP2−MP4(SDQ), and CCSD(T) methods (one page). Table of geometrical parameters of X-Beg (X = HO, F, Cl, or I) (one page). Cartesian coordinates of important species including transition states (29 pages). Figure of the transition state structures with imaginary frequency and the important movements of each nuclei in the imaginary frequency (4 pages). Figure of the optimized geometry and relative stabilities of PdI(Ph)$(PH_3)_2$ and Pd(OH)(Ph)$(PH_3)_2$ (one page). Figure of the electron population changes of the hydoxo, chloro, and fluoro systems (3 pages). This material is available free of charge via the Internet at http://pubs.acs.org.

JA040020R